

Convergence of an adaptive scheme for the one-dimensional Vlasov-Poisson system

*Martin Campos Pinto*¹ and *Michel Mehrenberger*²

Abstract

An adaptive semi-Lagrangian scheme for solving the Cauchy problem associated to the periodic one-dimensional Vlasov-Poisson system is proposed and analyzed. A key feature of our method is the accurate evolution of the adaptive mesh from one time step to the next one, based on the analysis of the local regularity and how it gets transported by the numerical flow. The accuracy of the scheme is monitored by a prescribed tolerance parameter ε which represents the local interpolation error at each time step, in the L^∞ metric. The numerical solutions are proved to converge in L^∞ towards the exact ones as ε and Δt tend to zero provided the initial data is Lipschitz and has a finite total curvature, or in other terms, that it belongs to $W^{1,\infty} \cap W^{2,1}$. The rate of convergence is in $\mathcal{O}(\Delta t^2 + \varepsilon/\Delta t)$, which should be compared to the results of Besse, who recently established [6] similar rates for a uniform semi-Lagrangian scheme, but requiring that the initial data are in C^2 . Several numerical tests illustrate the effectiveness of our approach for generating the optimal adaptive discretizations.

Key words. Fully adaptive scheme, semi-Lagrangian method, Cauchy problem, Vlasov-Poisson system, convergence rates, adaptive graded meshes, hierarchical finite elements, discrete curvatures.

AMS subject classifications. 65M12, 65M50, 82D10.

1 Introduction

The Vlasov-Poisson system

$$\partial_t f(t, x, v) + v \cdot \partial_x f(t, x, v) + E(t, x) \cdot \partial_v f(t, x, v) = 0, \quad (1.1)$$

$$\partial_x E(t, x) = \int_{\mathbb{R}} f(t, x, v) dv - 1 = \rho(t, x) \quad (1.2)$$

describes the evolution of a collisionless plasma of charged particles (electrons and ions, with normalized mass and charge constants), here in one dimension, in

¹Laboratoire Jacques-Louis Lions, UMR CNRS 7598, Université Pierre et Marie Curie, Paris

²Institut de Recherche Mathématique Avancée, UMR CNRS 7501, Université Louis Pasteur, Strasbourg

the case where the magnetic effects are neglected in the Lorentz force. The variables x and v denoting respectively the space position and the velocity, $f(t, \cdot, \cdot)$ is the electron probability distribution in phase space at time t . Here, it is assumed that the background (positive) ions distribution f_b satisfies $\int_{\mathbb{R}} f_b(t, x, v) dv = 1$, so that $-\rho$ may be seen as the total charge density in the Poisson equation (1.2) that couples the self-consistent electric field $-E$ with the electrons distribution f . In the sequel, we shall follow many authors in dropping the minus signs and refer to ρ and E as the charge density and the electric field.

The mathematical solutions to the Cauchy Problem given by (1.1), (1.2) and the initial data

$$f(0, x, v) = f_0 \tag{1.3}$$

have been studied for many years: the global existence in time of weak solutions to the multidimensional problem was first proved in 1973 by Arsen'ev [1], and we refer the reader to the further results (on weak and smooth solutions) of Batt [3], Horst [28, 29], Bardos and Degond [2], Schaeffer [36], Lions and Perthame [31], and to the review book of Glassey [24]. Because we are considering the one dimensional problem, and because our numerical scheme needs the initial solution to be in $W^{2,1}$, and hence continuous, we can use an earlier result of Iordanski [30] (later improved by and Cooper and Klimas [17]) who established in the early 60s global existence and uniqueness for classical (continuous) solutions in the one dimensional case.

Since the beginnings of numerical plasma simulation in the 60s, many techniques have been investigated, among which the Lagrangian “particle in cell” method (PIC) which consists of approximating the plasma by a finite number of macro-particles. The trajectories of these particles are computed from the characteristic curves $t \rightarrow (X(t; s, x, v), V(t; s, x, v))$ of the Vlasov equation (1.1) that are solutions of

$$\partial_t X(t) = V(t), \quad \partial_t V(t) = E(t, X(t)) \tag{1.4}$$

with initial values $X(s) = x$ and $V(s) = v$, whereas self-consistent fields are computed by gathering the charge and current densities of the particles on a mesh of phase space (see [9] for more details). For one dimensional simulations, Eulerian methods like finite difference methods, finite element methods and conservative flux balance methods have also been investigated, we refer to [23] for a fairly exhaustive review of the literature on numerical simulation of the Vlasov equation. For higher dimensional simulations, the PIC method was preferred to the grid based method due to their computational cost, in particular when fine scales were required to simulate accurately the developement of filamentations that often occurs in the phase space. Unfortunately, this method produces an inherent numerical noise that prevents from describing precisely the tail of the distribution function f , and in the late 90s, the increase of computational power allowed to handle two dimensional and even in some case three dimensional problems with grid based methods. Among these, the semi-Lagrangian scheme originally introduced by Cheng and Knorr [12] and reconsidered by Sonnendrücker, Roche, Bertrand and Ghizzo [38] consists of computing at each time step a finite element type solution on a given mesh of phase space by a backward characteristic method. It can be regarded as an attempt to combine

the advantages of both Eulerian and Lagrangian advection schemes in that it avoids the often too restrictive CFL condition as well as the distortion of the mesh that precisely occurs where the filamentation develops. More precisely, the method takes advantage of the conservation of the exact solution f along the characteristic curves (1.4) by defining a nonlinear evolution operator $\mathbb{S}_{\Delta t}$ as

$$\mathbb{S}_{\Delta t}f(t^n)(x, v) := f(t^n, \tilde{X}(t^n; t^{n+1}, x, v), \tilde{V}(t^n; t^{n+1}, x, v)) \simeq f(t^{n+1}, x, v) \quad (1.5)$$

where Δt is a uniform time step and $t^n = n\Delta t$. Here \tilde{X} and \tilde{V} are an approximation of X and V obtained by replacing in (1.4) the exact (unknown) field $E(X(t), t)$ by an approximated field computed from $f(t^n)$, which makes $\mathbb{S}_{\Delta t}$ *nonlinear*. This advection step is then coupled to the phase space discretization by a finite element type interpolation operator P . In order to regain computational efficiency, some adaptive versions of this semi-Lagrangian method have been recently developed in [37] and [7, 25], where the authors use moving phase-space grids or interpolatory wavelets of Deslaurier and Dubuc. The principle shared by these adaptive schemes is to use only the “necessary” grid points when simulating plasma beams with small structures that move rapidly through the phase space.

The use of adaptive multiresolution techniques for dealing with the numerical treatment of transport PDE’s has already a substantial history, from adaptive mesh refinement [4] to wavelet-like techniques [19, 15]. Certain schemes use multiscale adaptivity to accelerate the computation of the numerical solution which is still described on a uniform mesh [26, 27, 13, 33], while other schemes are based on the description of the numerical solution on an adaptive mesh [4, 5, 20, 21, 16, 35]. In these techniques, a key issue is to design the adaptive discretization in such a way that

1. The error between the numerical solution and the exact solution is *rigorously controlled by a prescribed tolerance*. We refer in particular to [16], in which this goal is achieved in the context of finite volume schemes for hyperbolic conservation laws.
2. The adaptive discretization for achieving this prescribed accuracy has *optimal complexity*. A possible benchmark to properly define and evaluate this notion of optimality is provided by *nonlinear approximation theory*, which describes the optimal trade-off between accuracy and complexity in terms of specific Besov-Sobolev smoothness properties of the solution, see in particular [19, 22, 15, 8].

In this paper, we propose a new adaptive semi-Lagrangian scheme, in which the first above described objective is achieved. We also give theoretical heuristics and numerical evidence that the adaptive grids generated by this scheme have optimal complexity. In this scheme, the adaptive mesh is evolved together with the solution but always remains into a particular class of hierarchical finite element triangulations. The notion of good adaptation of a mesh M to a given function g is meant here in the sense that the interpolation error $(I - P_M)g$ is smaller in the L^∞ norm than a prescribed tolerance ε . But whereas the design of M is well understood when g is known, predicting the mesh for a to-be-computed solution is a more difficult task. In our algorithm this is executed

in two steps: the first step uses the adaptive mesh at the previous time step together with the numerical transport flow in order to design a new adaptive mesh, and the second step slightly corrects this mesh by local refinement or coarsening based on the *a posteriori* analysis of the numerical solution obtained by the semi-Lagrangian approach on the intermediate mesh. This second step is crucial in order to control the accuracy of the numerical scheme, which depends on both the time step Δt and the tolerance ε .

The starting point of our work was a first version of a multiresolution adaptive semi-Lagrangian scheme proposed by Sonnendrücker and Cohen, which was implemented in 2003 at the Cemracs summer school in Luminy, see [11], yet without any rigorous analysis. Regarding the error estimates, we mainly drew our inspiration from the proof of convergence given by Besse in [6] for a uniform version of the semi-Lagrangian scheme, but had to change the spirit of it. We shall briefly explain why. The uniform scheme formally reads as

$$f_u^n \rightarrow f_u^{n+1} = P_h \mathbb{S}_{\Delta t} f_u^n,$$

where P_h denotes the interpolation operator on the finite element space of uniform mesh size h , and Besse decomposes the numerical error into

$$f(t^{n+1}) - f_u^{n+1} = [f(t^{n+1}) - \mathbb{S}_{\Delta t} f(t^n)] + (I - P_h) \mathbb{S}_{\Delta t} f(t^n) + P_h [\mathbb{S}_{\Delta t} f(t^n) - \mathbb{S}_{\Delta t} f_u^n].$$

Once given an estimate for the time discretization error $\|f(t^{n+1}) - \mathbb{S}_{\Delta t} f(t^n)\|_{L^\infty}$, the key point is to make use of the C^2 smoothness which is assumed for the exact solution, in order to estimate the projection error $\|(I - P_h) \mathbb{S}_{\Delta t} f(t^n)\|_{L^\infty}$. In contrast, denoting by M^n the mesh associated to the adaptive numerical solution f^n , the adaptive scheme formally reads as

$$f^n \rightarrow f^{n+1} = P_{M^{n+1}} \mathbb{S}_{\Delta t} f^n,$$

where the mesh M^{n+1} has been obtained from M^n by the above mentioned strategy. In order to incorporate this strategy in our analysis, we had to decompose the numerical error according to

$$f(t^{n+1}) - f^{n+1} = [f(t^{n+1}) - \mathbb{S}_{\Delta t} f(t^n)] + (I - P_{M^{n+1}}) \mathbb{S}_{\Delta t} f^n + [\mathbb{S}_{\Delta t} f(t^n) - \mathbb{S}_{\Delta t} f^n].$$

Unlike in the first decomposition, the interpolation error is now considered on $\mathbb{S}_{\Delta t} f^n$ which is less smooth than $\mathbb{S}_{\Delta t} f(t^n)$. We are then left to study the regularity of the numerical solutions and for this purpose, we introduce a discrete curvature measure $|\cdot|_\star$ that stands for a weak equivalent of the Sobolev $W^{2,1}$ semi-norm for continuous piecewise affine functions of \mathbb{R}^2 . Our resulting error estimates are then established under the sole assumption that the initial data is in $W^{1,\infty} \cap W^{2,1}$, while those of [6] assume C^2 smoothness. Note that for solutions with local singularities such as filamentations - for which adaptive discretizations are obviously needed - the C^2 norm is much higher than the $W^{2,1}$ norm.

Our paper starts in §2 with a brief reminder of the main properties of the exact solutions and of the time splitting scheme $\mathbb{S}_{\Delta t}$ of Cheng and Knorr. A new estimate is given for the corresponding time discretization error which only involves the $W^{1,\infty}$ smoothness. The strategy for generating the adaptive meshes

is then described in §3 together with the numerical scheme, and the main convergence result is stated, together with some remarks on the optimality of the method. Several properties of the adaptive meshes are established in §4, which are used in the proof of the convergence result given in §5. Several numerical tests are given in §6 which illustrate the effectiveness of our approach.

2 The continuous problem and its time discretization

Here is a more precise description of our problem. Following Besse in [6], we consider that the plasma is 1-periodic in the x direction. In other words, (1.1)-(1.3) hold for $x \in [0, 1]$ with boundary conditions

$$f(t, 0, v) = f(t, 1, v) \quad (2.6)$$

and

$$E(t, 0) = E(t, 1). \quad (2.7)$$

According to the Poisson equation (1.2), the latter is equivalent to

$$\int \rho(t, x) dx = \iint f(t, x, v) dx dv - 1 = 0 \quad (2.8)$$

(unless specified, the integrals in x and v are always taken respectively over $[0, 1]$ and all \mathbb{R}), which means that the plasma is globally neutral, and also implies that the global mass is conserved. Finally, we see that the electric field is defined up to a constant, so that we cannot have a well-posed problem unless we add a zero-mean electrostatic condition

$$\int E(t, x) dx = 0. \quad (2.9)$$

A classical way to read the Poisson equation (1.2) is to introduce the electrostatic potential $\varphi = \varphi(t, x)$ such that $E(t, x) = -\partial_x \varphi(t, x)$. Denoting by $G = G(x, y)$ the Green function associated to our problem, that is to say, for $y \in [0, 1]$, the solution of

$$\partial_{xx}^2 G(\cdot, y) = \delta(\cdot - y) \quad \text{on } [0, 1]$$

with periodic boundary conditions $G(0, y) = G(1, y)$, we obtain

$$E(t, x) = \int K(x, y) \left(\int f(t, y, v) dv - 1 \right) dy \quad (2.10)$$

where

$$K(x, y) = -\partial_x G(x, y) = \begin{cases} y - 1 & \text{if } 0 \leq x < y \\ y & \text{if } y \leq x \leq 1. \end{cases} \quad (2.11)$$

2.1 Existence of solutions

Let $\Omega = [0, 1] \times \mathbb{R}$. In our context, theorem 5 of Cooper and Klimas [17] reads as follows.

Theorem 2.1. *If $f_0 \in \mathcal{C}(\Omega)$ is positive, 1-periodic in x , compactly supported in v , and satisfies*

$$\iint f_0(x, v) dx dv - 1 = 0,$$

then there exists a unique solution (f, E) of (1.1)-(1.3), (2.6)-(2.9) on $[0, T]$. In addition, this solution is constant along the characteristic curves (1.4) and it satisfies both (2.10) and the Ampere law

$$\partial_t E(t, x) = - \int f(t, x, v) v dv + \bar{j} \quad (2.12)$$

where the mean current density \bar{j} is a constant defined by

$$\bar{j} = \iint f(t, x, v) v dv dx = \iint f_0(x, v) v dv dx. \quad (2.13)$$

2.2 Smoothness of the solutions

It is now well known that the solutions of the Vlasov-Poisson system satisfy uniform smoothness estimates for large (but finite) times. As an example of such result, the following lemma is found in [34].

Lemma 2.2. *If $f_0 \in W^{m,p}(\Omega)$ satisfies the hypothesis of theorem 2.1, the solution satisfies for any final time T :*

$$f \in L^\infty([0, T]; W^{m,p}(\Omega)).$$

In order to establish an error estimate for the time discretization, we shall need that the solution and the electric field have some regularity, and a sufficient requirement is that f_0 is Lipschitz - for the adaptive scheme to be well posed, we will later ask f_0 to be also in $W^{2,1}$. More precisely, we shall make use of the following lemma (*in the sequel, the capital letter C will denote a constant which value may vary at each occurrence, and which usually depends on some final time T and on the initial solution f_0*):

Lemma 2.3. *If $f_0 \in W^{1,\infty}(\Omega)$ satisfies the hypothesis of theorem 2.1, then for any final time $T < \infty$, the solution has a bounded support in the v direction*

$$Q(T) := \sup\{|v| : \exists x, \exists t \in [0, T], f(t, x, v) > 0\} \leq Q(0) + 2T \quad (2.14)$$

and it satisfies

$$\begin{aligned} \|f\|_{L^\infty([0,T]; W^{1,\infty}(\Omega))} &\leq C(T) \\ \|\partial_t f\|_{L^\infty([0,T]; L^\infty(\Omega))} &\leq C(T) \\ \|E\|_{L^\infty([0,T]; W^{2,\infty}([0,1]))} &\leq C(T) \\ \|\partial_t E\|_{L^\infty([0,T]; W^{1,\infty}([0,1]))} &\leq C(T) \\ \|\partial_{tt}^2 E\|_{L^\infty([0,T]; L^\infty([0,1]))} &\leq C(T). \end{aligned} \quad (2.15)$$

Proof. Because these smoothness estimates are very simple to obtain in the one dimensional case, we recall how they follow from the Vlasov-Poisson system. To begin with, we observe that

$$\|E\|_{L^\infty([0,T]; W^{1,\infty}([0,1]))} \leq C(T) \quad (2.16)$$

and

$$\|\partial_t E\|_{L^\infty([0,T];L^\infty([0,1]))} \leq C(T) \quad (2.17)$$

are established as soon as $f_0 \in \mathcal{C}(\Omega)$ (and they in fact are proved in [17]). Indeed, we see that the conservation of f along the characteristic curves (1.4) yields

$$0 \leq f \leq \|f_0\|_{L^\infty(\Omega)} \quad (2.18)$$

and

$$Q(T) - Q(0) \leq \sup_{(x,v) \in \Omega} \int_0^T |\partial_t V(t; 0, x, v)| dt \leq T \|E\|_{L^\infty([0,T];L^\infty([0,1]))}. \quad (2.19)$$

Using successively (2.10), (2.18) and (2.8), we have then

$$\|E(t)\|_{L^\infty([0,1])} \leq \|K\|_{L^\infty} \left(\iint |f(t, x, v)| dx dv + 1 \right) \leq 2, \quad (2.20)$$

and (2.14) follows from (2.19) together with this last bound. We derive then respectively from the Poisson (1.2) and the Ampere (2.12) equations

$$\|\partial_x E\|_{L^\infty([0,T];L^\infty([0,1]))} \leq Q(T) \|f_0\|_{L^\infty(\Omega)} + 1$$

and

$$\|\partial_t E\|_{L^\infty([0,T];L^\infty([0,1]))} \leq Q(T)^2 \|f_0\|_{L^\infty(\Omega)} + \bar{j},$$

which proves (2.16) and (2.17). Now if $f_0 \in W^{1,\infty}(\Omega)$, letting

$$\begin{cases} (X, V)(s) = (X, V)(s; t, x, v) \\ (X', V')(s) = (X, V)(s; t, x', v') \end{cases} \quad \text{and} \quad \begin{cases} e_x(s) = |X(s) - X'(s)| \\ e_v(s) = |V(s) - V'(s)|, \end{cases}$$

we have

$$\begin{aligned} |f(t, x, v) - f(t, x', v')| &= |f_0(X(0), V(0)) - f_0(X'(0), V'(0))| \\ &\leq |f_0|_{W^{1,\infty}(\Omega)} (e_x + e_v)(0). \end{aligned}$$

Computing from (1.4) that $|\dot{e}_x(s)| \leq e_v(s)$ and

$$|\dot{e}_v(s)| \leq |E(s, X(s)) - E(s, X'(s))| \leq \|\partial_x E\|_{L^\infty([0,T];L^\infty([0,1]))} e_x(s)$$

we see that (2.16) together with a Gronwall argument yield

$$\begin{aligned} (e_x + e_v)(0) &= (e_x + e_v)(t) - \int_0^t (\dot{e}_x + \dot{e}_v)(s) ds \\ &\leq (e_x + e_v)(t) + (1 + C(T)) \int_0^t (e_x + e_v)(s) ds \\ &\leq C(T) (e_x + e_v)(T) \\ &\leq C(T) (|x - x'| + |v - v'|). \end{aligned}$$

This shows that $f(t)$ indeed has uniform Lipschitz smoothness on $[0, T]$, so that $\|f\|_{L^\infty([0,T];W^{1,\infty}(\Omega))}$ is bounded, whereas

$$\|\partial_t f(t)\|_{L^\infty(\Omega)} \leq Q(T) \|\partial_x f(t)\|_{L^\infty(\Omega)} + \|E\|_{L^\infty([0,1])} \|\partial_v f(t)\|_{L^\infty(\Omega)}$$

follows readily from the Vlasov equation (1.1). Turning to the electric field, we first see by differentiating the Poisson equation (1.2) with respect to x and t that $\|\partial_{xx}^2 E\|_{L^\infty([0,T];L^\infty([0,1]))}$ and $\|\partial_{tx}^2 E(t)\|_{L^\infty([0,T];L^\infty([0,1]))}$ are respectively bounded by $Q(T)\|\partial_x f\|_{L^\infty([0,T];L^\infty(\Omega))}$ and $Q(T)\|\partial_t f\|_{L^\infty([0,T];L^\infty(\Omega))}$, while the bound on $\|\partial_{tt}^2 E\|_{L^\infty([0,T];L^\infty([0,1]))}$ is obtained by differentiating the Ampere equation (2.12) with respect to t . \square

2.3 Time discretization

Following [12], [38] and [6], we now describe a simple and accurate time splitting advection scheme $\mathbb{S}_{\Delta t}$. We recall that Δt is a uniform time step and write $t^n = n\Delta t$.

x and v transport operators. To any given advection field $\mathcal{F} : \Omega \rightarrow \mathbb{R}^2$, we associate a transport operator $\mathcal{T} : g \rightarrow g \circ \mathcal{F}^{-1}$ defined for any continuous function g . In particular, two one-directional advections are considered in the time splitting scheme:

$$\mathcal{F}_x : (x, v) \rightarrow (x + v\Delta t/2, v) \quad (2.21)$$

and

$$\mathcal{F}_v(h) : (x, v) \rightarrow (x, v + \Delta t \tilde{E}(h)(x)), \quad (2.22)$$

where h and $\tilde{E}(h)$ respectively denote an auxiliary density function and the associated electric field

$$\tilde{E}(h)(x) = \int K(x, y) \left(\int h(y, v) dv - 1 \right) dy. \quad (2.23)$$

We then let

$$\mathcal{T}_x : g \rightarrow g \circ \mathcal{F}_x^{-1}, \quad \mathcal{T}_v(h) : g \rightarrow g \circ \mathcal{F}_v(h)^{-1} \quad (2.24)$$

be the linear transport operators associated to \mathcal{F}_x and $\mathcal{F}_v(h)$ and finally denote by \mathcal{T}_v the *nonlinear* transport operator

$$\mathcal{T}_v : g \rightarrow \mathcal{T}_v(g)g. \quad (2.25)$$

The time splitting scheme $\mathbb{S}_{\Delta t}$ approximates then $f(t^{n+1})$ by

$$\mathbb{S}_{\Delta t} f(t^n) := \mathcal{T}_x \mathcal{T}_v \mathcal{T}_x f(t^n), \quad (2.26)$$

which corresponds to (1.5) with

$$\begin{cases} \tilde{X}(t^n; t^{n+1}, x, v) := x - v\Delta t + \Delta t^2/2 \tilde{E}(\mathcal{T}_x f(t^n))(x - v\Delta t/2) \\ \tilde{V}(t^n; t^{n+1}, x, v) := v - \Delta t \tilde{E}(\mathcal{T}_x f(t^n))(x - v\Delta t/2). \end{cases} \quad (2.27)$$

The following lemma establishes that the associated global time discretization error decays like Δt^2 .

Lemma 2.4. *If f_0 is in $W^{1,\infty}(\Omega)$, then*

$$\|f(t^{n+1}) - \mathbb{S}_{\Delta t} f(t^n)\|_{L^\infty} \leq C(T)\Delta t^3.$$

The proof is given in the appendix.

Remark 2.5. A similar result is shown in [6], with the stronger assumption that f_0 is in $C^2(\Omega)$.

Remark 2.6. The choice of using this time splitting scheme is mostly motivated by its simplicity (and its accuracy as well). It should be emphasized, however, that the adaptive space discretization scheme that we next describe can be applied to other types of time discretizations. For example, one could consider a unique transport operator of the form

$$\mathcal{T} : g \rightarrow g \circ \mathcal{F}(g)^{-1}$$

which combines the advection in the x and v variables.

3 The numerical scheme

Our adaptive scheme basically consists of three Lagrange-Projection steps which respectively follow the three advection steps of the time splitting. For each of them, the mesh M_i^n on which the intermediate solution f_i^n is known is first “transported” into a new one M_{i+1}^n , in such a way that determining $f_{i+1}^n := P_{M_{i+1}^n} \mathcal{T}_i f_i^n$ amounts to the computation of $\mathcal{T}_i f_i^n$ at the nodes of M_{i+1}^n . We shall now specify the rules for designing these adaptive meshes.

3.1 Adaptive discretization

Our space discretization is based on hierarchical finite elements. *Following the rather classical idea of combining good adaption qualities and a very simple underlying structure*, we will consider a particular class of adaptive triangulations that are associated to *graded dyadic quadrangulations* and which can also be seen as a particular case of the so called “newest vertex bisection” method described in [8] (we refer to [15] or [39] for more informations about hierarchical bases).

Adaptive dyadic quadrangulations. Let us first denote by \mathcal{Q}_ℓ the uniform quadrangulation made of all dyadic, square cells of resolution level $\ell \in \mathbb{N}$

$$\mathcal{Q}_\ell := \{ [j 2^{-\ell}, (j+1) 2^{-\ell}] \times [k 2^{-\ell}, (k+1) 2^{-\ell}] : j, k \in \mathbb{Z} \}$$

and by $\mathcal{Q} := \cup_\ell \mathcal{Q}_\ell$ the set of all dyadic quadrangles. Here no level is supposed to be lower than a prescribed $\ell_0 > 0$, and we shall consider that $\mathcal{Q}_\ell := \emptyset$ for any $\ell < \ell_0$. We observe then that the cells are embedded, so that each \mathcal{Q}_ℓ can be seen as a refinement of the smaller set $\mathcal{Q}_{\ell-1}$, and we obtain a quadtree structure by defining for any given $\alpha \in \mathcal{Q}$ of level $\ell(\alpha)$ its *children* cells as

$$\mathcal{C}(\alpha) := \{ \beta \in \mathcal{Q}_{\ell(\alpha)+1} : \beta \subset \alpha \},$$

and its parent cell as $\beta \in \mathcal{Q}_{\ell(\alpha)-1}$ such that $\alpha \subset \beta$. We also define the *ancestor* cells of α as

$$\mathcal{A}(\alpha) := \{ \beta \in \bigcup_{\ell < \ell(\alpha)} \mathcal{Q}_\ell : \beta \supset \alpha \}.$$

We will then call $\Lambda \subset \mathcal{Q}$ a *consistent tree* if it satisfies

$$\mathcal{Q}_{\ell_0} \subset \Lambda \quad \text{and} \quad \bigcup_{\beta \in \mathcal{A}(\alpha)} \mathcal{C}(\beta) \subset \Lambda \quad \text{for any } \alpha \in \Lambda.$$

This second property implies that no cell of Λ is partially refined, so that any $\alpha \in \Lambda$ satisfies $\mathcal{C}(\alpha) \cap \Lambda = \emptyset$ or $\mathcal{C}(\alpha) \subset \Lambda$. As a consequence, we observe that the *leaves* of Λ , that is the set

$$\mathcal{L}(\Lambda) := \{ \alpha \in \Lambda : \mathcal{C}(\alpha) \cap \Lambda = \emptyset \},$$

forms a partition of the phase space (except for the edges). We will say that $M \subset \mathcal{Q}$ is an *adaptive quadrangulation* if there is a consistent tree Λ such that $M = \mathcal{L}(\Lambda)$. In addition, M will be called *graded* if its local resolution has no “jumps”, or in other words, if two neighboring cells α and β (sharing at least one edge) satisfy $|\ell(\alpha) - \ell(\beta)| \leq 1$.

Remark 3.1. Imposing this graded condition is a reasonable requirement, since for any adaptive quadrangulation M , there exists a graded refinement M' of M that satisfies $\#(M') \leq C\#(M)$ with C an absolute constant (see lemma 2.4 in [18] for a proof).

Conforming triangulations. To any graded adaptive quadrangulation M of the above type, we shall now derive a conforming triangulation for the \mathcal{P}_1 interpolation to be well defined. We recall that a triangulation is said to be conforming if any edge of any triangle is either a subset of the boundary (when there is one), or an edge of another triangle. To do this, we construct a first triangulation \tilde{M}_t by splitting each cell $\alpha \in M$ in two triangles, with the following rule: if α is an upper left or a lower right child (of its parent cell), it is splitted into its lower left and upper right halves, and the splitting is symmetric in the other two cases. For this rule to be applied to the cells of the lowest level ℓ_0 , we can always consider a fictitious lower level $\ell_0 - 1$, so that each cell of level ℓ_0 has a parent cell (nevertheless, the way they are splitted does not matter much for the sequel). We can observe on figure 1 that the resulting \tilde{M}_t is nonconforming: since M is not uniform, it contains at least one cell α sharing an edge with two cells β and λ such that $\ell(\beta) = \ell(\lambda) = \ell(\alpha) + 1$. And if we denote by β_t and λ_t the two triangles resulting from the splitting of β and λ that share an edge with α , it is readily seen that they are not conforming with the adjacent triangle resulting from the splitting of α . But since M is graded, this is the only possible configuration where the triangles are nonconforming, and we see that a conforming triangulation M_t is simply obtained by merging any such couple of triangles (β_t, λ_t) .

To emphasize the simple structure of the original quadrangulation M compared to the associated conforming triangulation M_t , such a couple is represented on figure 2.

Piecewise affine interpolations. Because we are interested in L^∞ error estimates, it will be helpful that the projection operators cannot increase the L^∞ norm. We shall here consider \mathcal{P}_1 Lagrange interpolation which obviously meets this requirement. Denoting by $N(M_t)$ the vertices of M_t , and by

$$V_M := \{ g \in \mathcal{C}^0 : g|_K \in \Pi_1, \forall K \in M_t \}$$

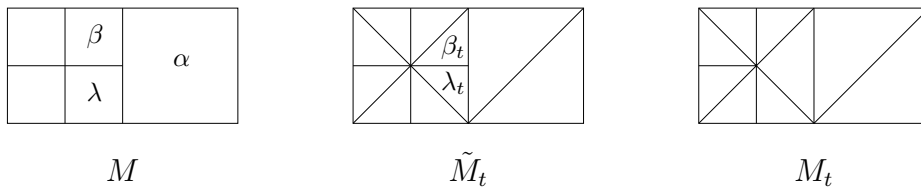


Figure 1: splitting of nonuniform cells and merging of nonconforming triangles.

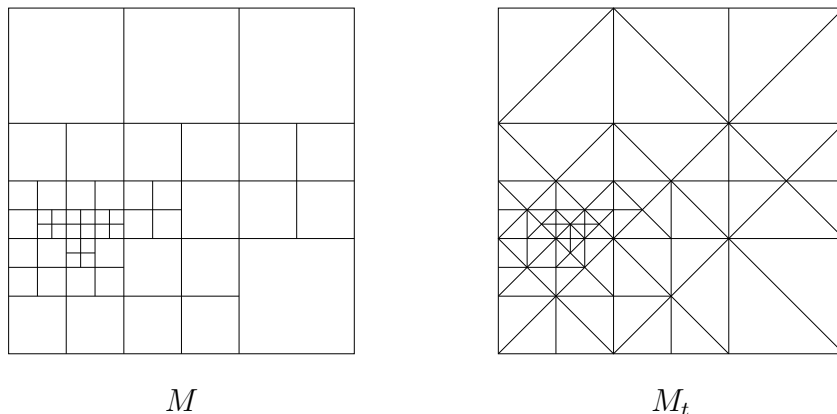


Figure 2: one graded quadrangulation and its associated conforming triangulation.

the associated finite element space, we let then P_M be the natural \mathcal{P}_1 interpolation associated to the conforming triangulation M_t . We may recall that for any continuous function g , $P_M g$ is the unique element of V_M that satisfies

$$P_M g = g \quad \text{on } N(M_t).$$

Remark 3.2. It is possible to use higher order \mathcal{P}_k Lagrange interpolation operators P_M^k associated to the same triangulation. They lead to similar adaptive scheme which might exhibit better results in practice, but for which we do not have a satisfactory error analysis.

3.2 Mesh operations

We now present the two mesh algorithms that appear in the adaptive scheme. *In the sequel, the word “mesh” will always refer to an adaptive quadrangulation, graded if nothing else is mentionned.* We begin by introducing two functionals that play a paramount role in the design of the meshes.

Discrete curvatures. In order to guarantee small interpolation errors, we will need to control the *amount of curvature* of the numerical solutions. For this purpose, we associate to any mesh M and any function g the quantity

$$\mu(g, M) := \sup_{\alpha \in M} \text{curv}(g, \alpha) \quad (3.28)$$

where $\text{curv}(g, \alpha)$ is a quantity which is equal to $|g|_{W^{2,1}(\alpha)}$ for $g \in W^{2,1}$. This quantity will be precisely defined in (4.55) and its definition will be extended to functions g which are not in $W^{2,1}$ but are continuous and piecewise affine on some arbitrary triangulation. The discrete curvature controls the error of \mathcal{P}_1 interpolation in the following sense: there exists a uniform constant C such that for all $\alpha \in M$ and for K a triangle of M_t contained in α , we have

$$\|g - P_M g\|_{L^\infty(K)} \leq C \text{curv}(g, \alpha). \quad (3.29)$$

We postpone to §4.2 the proof of this estimate.

Weighted Lipschitz semi-norm. In parallel with the local curvatures, we will need to control a second quantity, namely

$$\pi(g, M) := \sup_{\alpha \in M} 2^{-2\ell(\alpha)} |g|_{W^{1,\infty}(\alpha)}. \quad (3.30)$$

We now describe the main mesh algorithms.

Mesh adaptation. Given a function g for which μ and π are finite (such as a function of $W^{2,1} \cap W^{1,\infty}$, or a piecewise affine functions) and a prescribed tolerance $\varepsilon > 0$, we are interested in constructing a mesh $\mathbb{A}_\varepsilon(g)$, the smallest as possible, such that

$$\mu(g, \mathbb{A}_\varepsilon(g)) + \Delta t \pi(g, \mathbb{A}_\varepsilon(g)) \leq \varepsilon. \quad (3.31)$$

Since this is achieved by asking that

$$\nu(g, \alpha) := \text{curv}(g, \alpha) + \Delta t 2^{-2\ell(\alpha)} |g|_{W^{1,\infty}(\alpha)} \leq \varepsilon/2 \quad (3.32)$$

holds for any $\alpha \in \mathbb{A}_\varepsilon(g)$, a natural solution consists of performing adaptive splitting: starting from the root quadrangulation \mathcal{Q}_{ℓ_0} , any cell α for which (3.32) does not hold is refined into its four children cells, and this is performed recursively, so that the resulting $\tilde{\mathbb{A}}_\varepsilon$ is the smallest (non graded) mesh satisfying (3.31) (for sake of simplicity, we choose not to impose a maximal level L for the cells). We let then $\mathbb{A}_\varepsilon(g)$ be the smallest graded refinement of $\tilde{\mathbb{A}}_\varepsilon$.

Since $\mathbb{A}_\varepsilon(g)$ and M do not differ very much in practice, a more efficient algorithm (yielding the same mesh) consists of applying the above refinement process not on \mathcal{Q}_{ℓ_0} but rather on an intermediate mesh \tilde{M} constructed by derefining M in the following way: starting from the maximum level $\ell(M)$ of M , we set $\Lambda_{\ell(M)}^a := M$ and for any $\ell \leq \ell(M)$, let

$$\Lambda_{\ell-1}^a := \Lambda_\ell^a \setminus \{ \alpha \in \mathcal{C}(\beta) : \ell(\alpha) = \ell, \mathcal{C}(\beta) \subset \mathcal{L}(\Lambda_\ell^a) \text{ and } \nu(g, \beta) \leq \varepsilon/2 \}$$

up to $\tilde{M} := \Lambda_{\ell_0}^a$. This algorithm clearly guarantees (3.31) and *should allows us to control the cardinality of the resulting meshes* (see paragraph 3.5 and §6).

Mesh transport. Given an advection field \mathcal{F} , we now give a strategy for “transporting” any mesh M into a new one, denoted $\mathbb{T}(M, \mathcal{F})$, on which *it will be easy to control the error resulting from the interpolation of $g \circ \mathcal{F}^{-1}$, as soon as g is known* (for a precise statement of this important property, we refer to corollary 4.4 and lemma 4.13). Strictly speaking, $\mathbb{T}(\cdot, \mathcal{F})$ is *not* a transport

operator, since the new meshes always belong to the class of graded dyadic quadrangulations, but it *looks like* a transport operator. The method indeed consists of looking backwards at the local resolution of M : for any cell $\alpha \in \mathcal{Q}$, we let its *backward level in M* be the integer

$$\ell^*(M, \mathcal{F}, \alpha) := \max\{\ell(\beta) : \beta \in M, \mathcal{F}^{-1}(c_\alpha) \in \bar{\beta}\} \leq \ell(M), \quad (3.33)$$

where $c_\alpha = (x_\alpha, v_\alpha)$ is the center of α . Here $\bar{\beta}$ denotes the closure of the cell β . Setting then $\Lambda_{\ell_0}^t := \mathcal{Q}_{\ell_0}$, we proceed as for \mathbb{A}_ε by iterative splitting and obtain $\Lambda_{\ell+1}^t$ by refining in Λ_ℓ^t each cell whose backward level is larger than its own level. In other terms, we let

$$\Lambda_{\ell+1}^t := \Lambda_\ell^t \cup \{ \beta \in C(\alpha) : \alpha \in \Lambda_\ell^t, \ell^*(M, \mathcal{F}, \alpha) > \ell(\alpha) \}.$$

This is done up to the highest level $\ell(M)$ of M , and we finally let $\mathbb{T}(M, \mathcal{F})$ be the smallest graded refinement of the non graded $\mathbb{T}(M, \mathcal{F}) := \mathcal{L}(\Lambda_{\ell(M)}^t)$. An interesting property (stated in lemma 4.12) is that for the advection fields used in our scheme, the cardinality of the resulting mesh $\mathbb{T}(M, \mathcal{F})$ is of the same order as that of M .

3.3 Description of the adaptive scheme

We are now able to write the precise form of the numerical scheme (up to some definitions that are stated below). Since every intermediate numerical solution f_i^n belongs to some finite element space $V_{M_i^n}$, the reader should be aware that a complete numerical solution is a pair of the form (M^n, f^n) , and the adaptive numerical scheme is represented by a mapping

$$\mathbb{S}_{\Delta t, \varepsilon} : (M^n, f^n) \rightarrow (M^{n+1}, f^{n+1}).$$

For the sake of simplicity we shall write in the sequel $f^{n+1} = \mathbb{S}_{\Delta t, \varepsilon} f^n$, keeping in mind that the scheme actually operates on the couple (M^n, f^n) .

The initialization step. Using the adaption algorithm \mathbb{A}_ε , which can be viewed as a *compression algorithm*, we define the first solution pair (M^0, f^0) as

$$M^0 := \mathbb{A}_\varepsilon(f_0) \quad \text{and} \quad f^0 := P_{M^0} f_0. \quad (3.34)$$

We shall denote for the sequel $\mathbb{S}_\varepsilon^0 : g \rightarrow P_{\mathbb{A}_\varepsilon(g)} g$.

The four steps adaptive scheme. For any time step $n \geq 1$, we let then

$$M_1^n := \mathbb{T}(M^n, \mathcal{F}_x) \quad \text{and} \quad f_1^n := P_{M_1^n} \mathcal{T}_x f^n \quad (3.35a)$$

$$M_2^n := \mathbb{T}(M_1^n, \mathcal{F}_v^n) \quad \text{and} \quad f_2^n := P_{M_2^n} \mathbb{T}_{n+1} \mathcal{T}_v^n f_1^n \quad (3.35b)$$

$$M_3^n := \mathbb{A}_\varepsilon(f_2^n) \quad \text{and} \quad f_3^n := P_{M_3^n} f_2^n \quad (3.35c)$$

$$M^{n+1} := \mathbb{T}(M_3^n, \mathcal{F}_x) \quad \text{and} \quad f^{n+1} := P_{M^{n+1}} \mathcal{T}_x f_3^n \quad (3.35d)$$

where \mathcal{F}_x and \mathcal{T}_x are defined in section 2.3, \mathcal{F}_v^n is an approximation of the advection field $\mathcal{F}_v(f_1^n)$ of (2.22) which is defined below, \mathcal{T}_v^n is the associated transport operator, and \mathbb{T}_{n+1} is a soft truncation in the v -direction which is also defined below.

Summing up, we have

$$f^{n+1} = \mathbb{S}_{\Delta t, \varepsilon} f^n = P_{M^{n+1}} \mathcal{T}_x P_{M_3^n} P_{M_2^n} \mathbb{T}_{n+1} \mathcal{T}_v^n P_{M_1^n} \mathcal{T}_x f^n = (\mathbb{S}_{\Delta t, \varepsilon})^{n+1} \mathbb{S}_\varepsilon^0 f_0.$$

The numerical electric field E^n and the advection field \mathcal{F}_v^n . Rather than strictly following the time splitting scheme (2.26), which would amount in the application of \mathcal{T}_x , $\mathcal{T}_v(f_1^n)$ and again \mathcal{T}_x , we slightly modify $\mathcal{F}_v(f_1^n)$ into \mathcal{F}_v^n , and apply $\mathcal{T}_v^n : g \rightarrow g \circ (\mathcal{F}_v^n)^{-1}$ instead of $\mathcal{T}_v(f_1^n)$. This is due to two different reasons: the first one is that the forthcoming error analysis is based on estimations of local curvature measures that are established for *piecewise affine functions*, and $\tilde{E}(g)$ being not piecewise affine (even if g is), the associated transport operator $\mathcal{T}_v(g)$ does not preserve the piecewise affine structure. The second reason lies in the lack of conservativity of the scheme, which derives from the lack of conservativity of the \mathcal{P}_1 interpolations. Since $\iint f_1^n$ may differ from $\iint f_0$, the condition (2.8) has no reason to be fulfilled by f_1^n , which makes $\tilde{E}(f_1^n)$ nonperiodic, as well as $\mathcal{F}_v(f_1^n)$. As a consequence, we first correct $\tilde{E}(f_1^n)$ into the Lipschitz 1-periodic electric field \tilde{E}^n by setting

$$\tilde{E}^n(x) = \tilde{E}(f_1^n)(\{x\}) + \{x\}[\tilde{E}(f_1^n)(0) - \tilde{E}(f_1^n)(1)] \quad (3.36)$$

where $\{x\}$ is the *fractional part* of x , and then let E^n be the piecewise affine interpolation of \tilde{E}^n on

$$\Gamma^n := N_x(M_1^n), \quad (3.37)$$

where the set

$$N_x(M) := \bigcup_{\alpha \in M} \partial(\alpha_x) \quad (3.38)$$

is nothing but the projection on the x axis of the nodes of a given mesh M . The advection field \mathcal{F}_v^n is then defined by

$$\mathcal{F}_v^n : (x, v) \rightarrow (x, v + \Delta t E^n(x)),$$

which should be seen as a correction of $\mathcal{F}_v(f_1^n) : (x, v) \rightarrow (x, v + \Delta t \tilde{E}(f_1^n)(x))$.

Remark 3.3. Applying \mathcal{T}_v^n (or \mathcal{F}_v^n) amounts to computing $\{\tilde{E}^n(x_i)\}_{x_i \in \Gamma^n}$. According to (3.36), (2.23) and writing $\rho_1^n = \int f_1^n dv - 1$, this is equivalent to determining the values

$$\tilde{E}(f_1^n)(x_i) = \int_0^1 K(x_i, y) \rho_1^n(y) dy = \int_0^1 y \rho_1^n(y) dy - \int_{x_i}^1 \rho_1^n(y) dy, \quad (3.39)$$

where the second equality comes from (2.11). Now because any vertex of any affine piece of f_1^n is of the form (x_i, v) with $x_i \in \Gamma^n$, a little algebra shows that ρ_1^n is quadratic between two nodes of Γ^n . Moreover, we see that its computational cost is on the order of $\#(M_1^n)$, and since $\#(\Gamma^n) \leq \#(M_1^n)$, it follows from (3.39) that applying \mathcal{T}_v^n achieves a computational cost of order $\#(M_1^n)$.

Remark 3.4. In fact, we will need in the sequel (see lemma 4.13) that the “intermediate” field \tilde{E}^n is in $W^{2,\infty}$. Rather surprisingly, this is also ensured by (3.36). As a matter of fact, we have

$$(\tilde{E}^n)'(0^+) - (\tilde{E}^n)'(0^-) = \tilde{E}(f_1^n)'(0^+) - \tilde{E}(f_1^n)'(0^-) = \int_0^1 f_1^n(0, v) - f_1^n(1, v) dv = 0$$

since f_1^n is, by construction, 1-periodic in x .

Soft truncation in v . We end this section by discussing the issue of controlling the support of the numerical solutions in the v direction, that is quantity

$$\Sigma_v(f^n) := \sup\{|v| : \exists x, f^n(x, v) > 0\}. \quad (3.40)$$

In section 2.2, the quantity $Q(t)$ was defined to bound the support of the exact solutions, and it has been shown that $Q(t^n) \leq Q(0) + 2t^n$. But turning to f^n , we observe that $\Sigma_v(f^n)$ can grow by a coarse mesh step $2^{-\ell_0}$ at each interpolation step, so that there is no reason for $\Sigma_v(f^n)$ to be bounded independently of the time step Δt . Nevertheless, an priori bound is required in order to estimate the numerical electric field E^n (apart from the fact that it also provides a maximal size of the computational mesh) as it will appear below. To remedy this problem, we let $Q_n := Q(0) + 2n\Delta t$ and then

$$\hat{Q}_n := 2^{-\ell_0}(\lceil 2^{\ell_0} Q_n \rceil + 1) \geq Q_n + 2^{-\ell_0} \quad (3.41)$$

be the lowest multiple of $2^{-\ell_0}$ larger than $Q_n + 2^{-\ell_0}$. In particular, it satisfies $\hat{Q}_n \leq Q_n + 2 \cdot 2^{-\ell_0}$ (the reasons for choosing such a \hat{Q}_n will appear later on, see in particular the remarks below). The soft truncation operator \mathbb{T}_n is then defined as

$$\mathbb{T}_n g(x, v) = \begin{cases} 0 & \text{if } |v| > \hat{Q}_n + 2^{-\ell_0} \\ g(x, -\hat{Q}_n)(\hat{Q}_n + 2^{-\ell_0} + v)2^{\ell_0} & \text{if } -\hat{Q}_n - 2^{-\ell_0} \leq v < -\hat{Q}_n \\ g(x, v) & \text{if } -\hat{Q}_n \leq v \leq \hat{Q}_n \\ g(x, \hat{Q}_n)(\hat{Q}_n + 2^{-\ell_0} - v)2^{\ell_0} & \text{if } \hat{Q}_n < v \leq \hat{Q}_n + 2^{-\ell_0} \end{cases} \quad (3.42)$$

Using this operator, we shall establish in §5 that any numerical solution has its support bounded by

$$\tilde{\Sigma}_v := Q(0) + 2T + 7 \cdot 2^{-\ell_0} \leq \Sigma_v(f_0) + 2T + 7. \quad (3.43)$$

Remark 3.5. Since $Q_n \geq Q(t^n)$, it is readily seen that $f(t^n)$ vanishes outside $\Omega_n := \mathbb{R} \times [-Q_n, Q_n]$ and outside $\hat{\Omega}_n := \mathbb{R} \times [-\hat{Q}_n, \hat{Q}_n]$ as well, since $\Omega_n \subset \hat{\Omega}_n$ follows from (3.41).

Remark 3.6. \hat{Q}_n being a multiple of $2^{-\ell_0}$ implies that any dyadic quadrangular cell (of any mesh M) is either in $\hat{\Omega}_n$ or in $(\hat{\Omega}_n)^c$. This also holds for the triangles of M_t , and therefore any continuous g satisfies the localized maximum principles

$$\|P_M g\|_{L^\infty(\hat{\Omega}_n)} \leq \|g\|_{L^\infty(\hat{\Omega}_n)} \quad \text{and} \quad \|P_M g\|_{L^\infty((\hat{\Omega}_n)^c)} \leq \|g\|_{L^\infty((\hat{\Omega}_n)^c)}. \quad (3.44)$$

Moreover, we have for any n , M and g

$$(P_M g)|_{\hat{\Omega}_n} = P_M(g|_{\hat{\Omega}_n}), \quad (\mathcal{T}_x g)|_{\hat{\Omega}_n} = \mathcal{T}_x(g|_{\hat{\Omega}_n}) \quad \text{and} \quad (\mathbb{T}_n g)|_{\hat{\Omega}_n} = g|_{\hat{\Omega}_n}. \quad (3.45)$$

3.4 Main Theorem

Here is our *a priori global error estimate* between the adaptive solutions and the exact ones.

Theorem 3.7. *If the initial data $f_0 \in W^{1,\infty}(\Omega) \cap W^{2,1}(\Omega)$ meets the hypothesis of theorem 2.1, then for any final time $T = N\Delta t$ there is a constant $C = C(T, f_0)$ for which the adaptive numerical solution $f^N := (\mathbb{S}_{\Delta t, \varepsilon})^N \mathbb{S}_\varepsilon^0 f_0$ satisfies*

$$\|f(T) - f^N\|_{L^\infty} \leq C(\Delta t^2 + \varepsilon/\Delta t) \quad (3.46)$$

provided ε and Δt verify

$$\varepsilon^{1/2} \leq \Delta t \leq [8(\tilde{\Sigma}_v \|f_0\|_{L^\infty} + 1)]^{-1}, \quad (3.47)$$

with $\tilde{\Sigma}_v$ defined in (3.43).

Remark 3.8. The above condition $\varepsilon \leq \Delta t^2$ can be replaced by $\varepsilon \leq C\Delta t^2$ for some constant C . In addition, we observe that balancing (3.46) gives $\varepsilon = \Delta t^3$ and

$$\|f(T) - f^N\|_{L^\infty} \leq C(T) \Delta t^2 = C(T) \varepsilon^{2/3}.$$

As mentioned in the introduction, the proof of theorem 3.7 is based on decomposing the numerical error into

$$f(t^{n+1}) - f^{n+1} = [f(t^{n+1}) - \mathbb{S}_{\Delta t} f(t^n)] + (\mathbb{S}_{\Delta t} - \mathbb{S}_{\Delta t, \varepsilon}) f^n + [\mathbb{S}_{\Delta t} f(t^n) - \mathbb{S}_{\Delta t} f^n]$$

Apart from the first term which is the time discretization error estimated in lemma 2.4, and the third term which must be treated carefully since $\mathbb{S}_{\Delta t}$ is a nonlinear transport operator, we see that the error analysis relies on the study of the error term $\|(\mathbb{S}_{\Delta t} - \mathbb{S}_{\Delta t, \varepsilon}) f^n\|_{L^\infty}$. This term can be seen as a *space discretization error* that decomposes into the four interpolation errors corresponding to the four steps of the scheme, namely $\|(I - P_{M_1^n}) \mathcal{T}_x f^n\|_{L^\infty}$, $\|(I - P_{M_2^n}) \mathcal{T}_v^n f_1^n\|_{L^\infty}$, $\|(I - P_{M_3^n}) f_2^n\|_{L^\infty}$ and $\|(I - P_{M^{n+1}}) \mathcal{T}_v^n f_3^n\|_{L^\infty}$. Section 4 is devoted to finding a priori estimates for these interpolation errors.

3.5 Towards a complexity result

As a matter of fact, the above theorem is not completely satisfactory since it does not provide any estimate of the computational cost of the scheme, and therefore fails in proving a real gain of efficiency of the adaptive method compared to the uniform one. In both cases, the complexity is shown to be of the same order than the cardinality of the computational meshes. More precisely, denoting by \mathbf{N} the maximal cardinality of all the meshes used in the scheme, the complexity of one time step is of order \mathbf{N} in the uniform case, and according to the description of the mesh operations \mathbb{A}_ε , \mathbb{T} , and the remark 3.3 about the computational cost of E^n , it is of order $\mathbf{N} \log \mathbf{N}$ in the adaptive one. The natural question is thus: *does the adaptive scheme offers a better trade-off between N and the L^∞ error?* In [6], Besse shows that the L^∞ error e_u induced by the uniform scheme decays like $h^{4/3} = \Delta t^2$, h being the uniform space step. In this case $N \sim h^{-2}$ and we therefore obtain

$$e_u \leq C \mathbf{N}^{-2/3}. \quad (3.48)$$

According to remark 3.8, we see that the L^∞ error e_a induced by our adaptive scheme decays like $\varepsilon^{2/3} = \Delta t^2$, and we are left to understand the correlation between the parameter ε and the maximum cardinality \mathbf{N} of the adaptive meshes. This correlation can be heuristically described as follows: ideally, the adaptive splitting strategy $\mathbb{A}_\varepsilon(g)$ aims at building a mesh such that the total curvature on each triangle K of the adaptive triangulation is exactly of the order ε in order to control the interpolation error in the L^∞ norm. We indeed look for the smallest possible mesh such that

$$\|g - P_M g\|_{L^\infty(K)} \leq C |g|_{W^{2,1}(K)} \leq C \varepsilon, \quad (3.49)$$

according to (3.29) (in this heuristic argument, we have neglected the influence of the term $\Delta t \pi(g, \mathbb{A}_\varepsilon(g))$ on the complexity of the adaptive mesh). Let us therefore assume for a while that the total curvature $|g|_{W^{2,1}(K)}$ is not only bounded by above by ε , but also by below, say by $c\varepsilon$ with c a fixed constant. It would then readily follow that

$$N \leq C|g|_{W^{2,1}(\Omega)}\varepsilon^{-1}. \quad (3.50)$$

Therefore, provided that we can prove that the $W^{2,1}$ norm (or rather its weak version defined further by (4.54)) of the numerical solution remains bounded, we would obtain an error estimate of the type

$$e_a \leq C N^{-2/3}. \quad (3.51)$$

Note that this is not identical to (3.48), since it is achieved for solutions which are only in $W^{2,1}(\Omega)$ instead of $C^2(\Omega)$. It thus reveals that the adaptive scheme might perform substantially better than the uniform scheme when the exact solution is not C^2 or has very large C^2 norm.

At the present stage, we do not know how to rigorously establish (3.51) which may actually not hold without some slight additional assumptions. For example, it is proved in the survey article of DeVore [22] that similar adaptive splitting strategies have the optimal convergence rate provided that the second derivatives are not only bounded in L^1 but also in $L \log L$. Nevertheless, this raises the issue of estimating the growth of the total curvature $|f^n|_{\star(\Omega)}$ of the numerical solution. A partial result obtained in [10] constructs for any given triangulation \mathcal{T} a total curvature measure $|\cdot|_{\mathcal{T},\star(\Omega)}$ that is diminished by the \mathcal{P}_1 interpolation associated to any uniform refinement of \mathcal{T} .

4 Some properties of the adaptive discretization

Not surprisingly, our analysis of the discretization is driven by interpolation error estimates of the form

$$\|(I - P_M)g\|_{L^\infty} \leq C|g|_{X,M} \quad (4.52)$$

where the semi-norm $|\cdot|_{X,M}$ makes use of the local curvatures of the function g . If $g \in W^{2,1}$, for instance, it is shown below that inequality (4.52) holds with

$$|g|_{X,M} = \sup_{K \in \mathcal{M}_t} |g|_{W^{2,1}(K)}. \quad (4.53)$$

In the following, we denote by V the space of all continuous functions which are piecewise affine on an arbitrary conforming triangulation.

4.1 Smoothness of piecewise affine functions

In the context of \mathcal{P}_1 approximations, we would like to apply inequality (4.52) to the functions of V , but this cannot be achieved with (4.53). Indeed, the second derivatives of any such g are Dirac distributions supported on the edges of the associated triangulation, and hence are not in L^1 . Nevertheless, we see that on any bounded open domain ω they have a finite *total mass*

$$\int_\omega |\partial_{yz}^2 g| = \sup_{\substack{\varphi \in C_c^\infty(\omega) \\ \|\varphi\|_{L^\infty} \leq 1}} \left| \int_\omega \partial_y g \partial_z \varphi \right|$$

(y and z denoting either x or v). We can therefore relax the $W^{2,1}$ semi-norm into

$$|g|_{W^*(\omega)} := \int_{\omega} |\partial_{xx}^2 g| + |\partial_{xv}^2 g| + |\partial_{vv}^2 g|, \quad (4.54)$$

and consider the space W^* of any g such that $|g|_{W^*} := |g|_{W^*(\Omega)}$ is finite. Since $\mu_g := |\partial_{xx}^2 g| + |\partial_{xv}^2 g| + |\partial_{vv}^2 g|$ is a Borel measure, we extend the definition of $|g|_{W^*(\omega)}$ to any measurable set ω as $\mu_g(\omega)$. In the following we shall only consider the situation where ω is a closed curve or polygonal, in which case $\mu_g(\omega)$ possibly includes non-zero contributions from the edges of ω .

Definition of discrete curvatures. The new space W^* (that can be seen as the functions of bounded total curvature, in analogy to the functions of bounded total variation) now contains V and we can define the functional $\text{curv}(\cdot, \alpha)$ involved in (3.28) by

$$\text{curv}(g, \alpha) := |g|_{W^*(\alpha)}. \quad (4.55)$$

In order to simplify the forthcoming analysis of the discretization errors, we shall introduce another semi-norm for the piecewise affine functions: denoting by $\mathcal{E}(g)$ the edges of any $g \in V$, we let the *discrete curvature* of g on any closed polygonal domain (or curve) ω be defined by

$$|g|_{\star(\omega)} := \sum_{\gamma \in \mathcal{E}(g)} |\gamma \cap \omega| \|[Dg]_{\gamma}\|, \quad (4.56)$$

where $|\cdot|$ is the one-dimensional Hausdorff measure, $[Dg]_{\gamma}$ is the (constant) jump of the gradient vector $(\partial_x g, \partial_v g)$ on the edge γ and $\|\cdot\|$ denotes the ℓ^2 norm in \mathbb{R}^2 . Denoting by $\mathbf{n} = (\mathbf{n}_x, \mathbf{n}_v)$ the normal unit vector to γ (up to its sign), we can observe that the continuity of g yields

$$[\partial_x g]_{\gamma} \mathbf{n}_v = [\partial_v g]_{\gamma} \mathbf{n}_x \quad (4.57)$$

and hence

$$[Dg]_{\gamma} = [\partial_{\mathbf{n}} g]_{\gamma} \mathbf{n} = [\partial_x g \mathbf{n}_x + \partial_v g \mathbf{n}_v]_{\gamma} \mathbf{n}. \quad (4.58)$$

The equivalence between (4.54) and (4.56) is established by the following lemma.

Lemma 4.1. *For any closed polygonal domain ω and any $g \in V$, we have*

$$|g|_{\star(\omega)} \leq |g|_{W^*(\omega)} \leq 3/2 |g|_{\star(\omega)}. \quad (4.59)$$

Proof. We shall consider a particular closed polygonal ω that only contains one edge γ of $\mathcal{E}(g)$; the general case follows easily. After a little algebra, we find in this case that $\mu_g|_{\omega} = (|[\partial_x g]_{\gamma} \mathbf{n}_x| + |[\partial_x g]_{\gamma} \mathbf{n}_v| + |[\partial_v g]_{\gamma} \mathbf{n}_v|) \delta_{\gamma}$, hence

$$|g|_{W^*(\omega)} = |\gamma| (|[\partial_x g]_{\gamma} \mathbf{n}_x| + |[\partial_x g]_{\gamma} \mathbf{n}_v| + |[\partial_v g]_{\gamma} \mathbf{n}_v|). \quad (4.60)$$

On the other hand, we see that (4.58) gives $|g|_{\star(\omega)} = |\gamma| |[\partial_x g]_{\gamma} \mathbf{n}_x + [\partial_v g]_{\gamma} \mathbf{n}_v|$, so that the left inequality in (4.59) is obvious. Assuming then $\mathbf{n}_x \neq 0$ (which is always possible, up to a swap between x and v), we infer from (4.57) that

$$\begin{aligned} |\gamma|^{-1} |g|_{W^*(\omega)} &= |[\partial_x g]_{\gamma}| (|\mathbf{n}_x| + |\mathbf{n}_v| + \mathbf{n}_v^2 |\mathbf{n}_x|^{-1}) = |[\partial_x g]_{\gamma}| |\mathbf{n}_x|^{-1} (1 + |\mathbf{n}_x \mathbf{n}_v|) \\ &\leq 3/2 |[\partial_x g]_{\gamma}| |\mathbf{n}_x|^{-1} = 3/2 |[\partial_x g]_{\gamma}| |\mathbf{n}_x + \mathbf{n}_v^2 \mathbf{n}_x^{-1}| = 3/2 |\gamma|^{-1} |g|_{\star(\omega)} \end{aligned}$$

where we have used that $|\mathbf{n}_x \mathbf{n}_v| \leq 1/2$ and again (4.57) in the last equality. This establishes the right inequality of (4.59) and completes the proof. \square

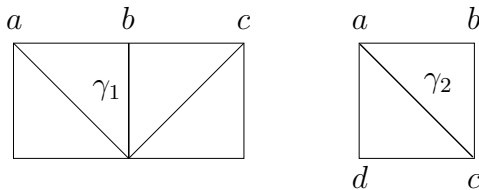


Figure 3: two type of edges for computing discrete curvatures.

Remark 4.2. When g belongs to some \mathcal{P}_1 finite element space $V_{M'}$, the quantity $\text{curv}(g, \alpha)$ is very straightforward to compute. As a matter of fact, we first verify that up to some local refinements, there are only two types of edges in the cell α where μ_g is non-zero, namely γ_1 and γ_2 represented on figure 3, According to (4.60), we have then

$$|g|_{W^*(\gamma)} = \mu_g(\gamma) = \begin{cases} |g(a) - 2g(b) + g(c)| & \text{if } \gamma = \gamma_1 \\ 3|g(a) - g(b) + g(c) - g(d)| & \text{if } \gamma = \gamma_2 \end{cases}$$

and $\text{curv}(g, \alpha)$ amounts to the sum of these curvatures.

4.2 Properties of the interpolation operators

We first recall a classical approximation result.

Lemma 4.3 (local interpolation error). *For any open triangle K and any $g \in W^*$, the local affine interpolation P_K satisfies*

$$\|g - P_K g\|_{L^\infty(K)} \leq C |g|_{W^*(K)} \quad (4.61)$$

where the constant C depends on the shape of K , but not on its size.

Proof. This estimate is a classical finite element result. Its proof relies on two main steps: the first one is the continuous embedding

$$\|g\|_{L^\infty(K)} \leq C \|g\|_{W^{2,1}(K)}, \quad (4.62)$$

and the second one is the equivalence between $\|g - P_K g\|_{W^{2,1}(K)}$ and $|g|_{W^{2,1}(K)}$ (see for instance [32] or [14]). This proves (4.61) with the $W^{2,1}$ semi-norm, now introducing the mollifier $\rho_\eta = \eta^{-2} \mathbb{1}_{\{(x,v):|x|+|v|\leq\eta\}}$ and letting η tend to zero in $g_\eta = g * \rho_\eta \in W^{2,1}$ shows that (4.61) also holds. Finally, one easily check the invariance of C by the isotropic scaling $K_\lambda = \lambda K$ using the change of variable $g_\lambda(x, v) = g(x/\lambda, v/\lambda)$. \square

According to this estimate, it is readily seen that inequality (4.52) indeed holds with (4.53), now because any triangle in M_t overlaps at most two quadrangles in M , we see that (4.52) also holds when $|g|_{X,M}$ is the quantity $\mu(M, g)$ given by (3.28). Let us write this as a corollary.

Corollary 4.4 (adaptive interpolation error). *For any graded mesh M and any $g \in W^*$, the piecewise affine interpolation P_M satisfies*

$$\|g - P_M g\|_{L^\infty} \leq C \mu(M, g) \quad (4.63)$$

where C is an absolute constant.

Remark 4.5. Using this simple estimate, we see that the initial numerical solution f^0 given by (3.34) satisfies $\|f^0 - f_0\|_{L^\infty} \leq C\varepsilon$ for any $f_0 \in W^*$.

We will also need that the interpolation operators do not increase the $W^{1,\infty}$ semi-norm, with the following convention:

$$|g|_{W^{1,\infty}} := \|\partial_x g\|_{L^\infty} + \|\partial_v g\|_{L^\infty}.$$

We shall underline that this is not an obvious property, for it is not satisfied with any adaptive triangulation.

Lemma 4.6 (Lipschitz diminishing). *For any mesh M and any $g \in W^{1,\infty}$, the interpolation operator P_M satisfies*

$$|P_M g|_{W^{1,\infty}} \leq |g|_{W^{1,\infty}}. \quad (4.64)$$

Proof. Let K be a triangle of M_t : either it comes from a simple quadrangle splitting, or it has been obtained by merging two nonconforming triangles K_1 and K_2 of \tilde{M}_t . In the first case, K has two edges parallel with the x and the v axis, and it is readily seen that $\|\partial_x P_M g\|_{L^\infty(K)}$ and $\|\partial_v P_M g\|_{L^\infty(K)}$ are respectively bounded by $\|\partial_x g\|_{L^\infty(K)}$ and $\|\partial_v g\|_{L^\infty(K)}$, so that

$$|P_M g|_{W^{1,\infty}(K)} \leq |g|_{W^{1,\infty}(K)} \quad (4.65)$$

is obvious. In the second case, we let $\tilde{g} := P_{\{K_1, K_2\}} g$ be the interpolation of g on the conforming subset $\{K_1, K_2\}$ of \tilde{M}_t . If the edge between K_1 and K_2 is parallel to the x axis, we have $\partial_x \tilde{g}|_{K_1} = \partial_x \tilde{g}|_{K_2}$.

$$\begin{aligned} \partial_x P_M g|_K &= (2\partial_x \tilde{g}|_{K_1} - \partial_v \tilde{g}|_{K_1} + \partial_v \tilde{g}|_{K_2}) / 2 \\ \partial_v P_M g|_K &= (\partial_v \tilde{g}|_{K_1} + \partial_v \tilde{g}|_{K_2}) / 2. \end{aligned}$$

Since $\partial_x P_M g$ and $\partial_v P_M g$ are constant on K , this yields

$$\begin{aligned} |P_M g|_{W^{1,\infty}(K)} &= \|\partial_x P_M g\|_{L^\infty(K)} + \|\partial_v P_M g\|_{L^\infty(K)} \\ &\leq \max(|\partial_x P_M g|_K + \partial_v P_M g|_K|, |\partial_x P_M g|_K - \partial_v P_M g|_K|) \\ &\leq \|\partial_x \tilde{g}\|_{L^\infty(K)} + \|\partial_v \tilde{g}\|_{L^\infty(K)} = |\tilde{g}|_{W^{1,\infty}(K)} \end{aligned}$$

and a symmetric argument shows that this inequality also holds in the case when the edge between K_1 and K_2 is parallel to the v axis. Using then (4.65), we have in any case

$$|P_M g|_{W^{1,\infty}(K)} \leq |\tilde{g}|_{W^{1,\infty}(K)} = \max_{i=1,2} |\tilde{g}|_{W^{1,\infty}(K_i)} \leq \max_{i=1,2} |g|_{W^{1,\infty}(K_i)} = |g|_{W^{1,\infty}(K)}$$

which completes the proof. \square

We finally state the following lemma, which proof does not raise any particular difficulty.

Lemma 4.7 (μ - and π -stability). *For any mesh M and any $g \in V$, the interpolation operator P_M satisfies*

$$\mu(P_M g, M) \leq C\mu(g, M) \quad (4.66)$$

and

$$\pi(P_M g, M) \leq C\pi(g, M) \quad (4.67)$$

for some absolute constants C .

4.3 Smoothness of the transported densities

We shall now give some estimates concerning the smoothness of the densities transported by \mathcal{T}_x and \mathcal{T}_v^n (we recall that the latter is defined in section 3.3 and calls for both interpolation grid Γ^n and intermediate field \tilde{E}^n). The main result is:

Lemma 4.8. *If g is piecewise affine, then $\mathcal{T}_x g$ and $\mathcal{T}_v^n g$ also are. In addition, we have on any cell α*

$$|\mathcal{T}_x g|_{W^{1,\infty}(\alpha)} \leq (1 + \Delta t/2) |g|_{W^{1,\infty}(\mathcal{F}_x^{-1}(\alpha))} \quad (4.68)$$

$$|\mathcal{T}_v^n g|_{W^{1,\infty}(\alpha)} \leq (1 + \Delta t |\tilde{E}^n|_{W^{1,\infty}}) |g|_{W^{1,\infty}((\mathcal{F}_v^n)^{-1}(\alpha))} \quad (4.69)$$

$$|\mathcal{T}_x g|_{\star(\alpha)} \leq (1 + \Delta t/2)^2 |g|_{\star(\mathcal{F}_x^{-1}(\alpha))}. \quad (4.70)$$

If, in addition, α belongs to some graded mesh M verifying

$$N_x(M) \subset \Gamma^n, \quad (4.71)$$

the transported density $\mathcal{T}_v^n g$ satisfies

$$\begin{aligned} |\mathcal{T}_v^n g|_{\star(\alpha)} &\leq (1 + \Delta t |\tilde{E}^n|_{W^{1,\infty}})^2 |g|_{\star((\mathcal{F}_v^n)^{-1}(\alpha))} \\ &\quad + 5 \cdot 2^{-2\ell(\alpha)} \Delta t |\tilde{E}^n|_{W^{2,\infty}} \|\partial_v g\|_{L^\infty((\mathcal{F}_v^n)^{-1}(\alpha))}. \end{aligned} \quad (4.72)$$

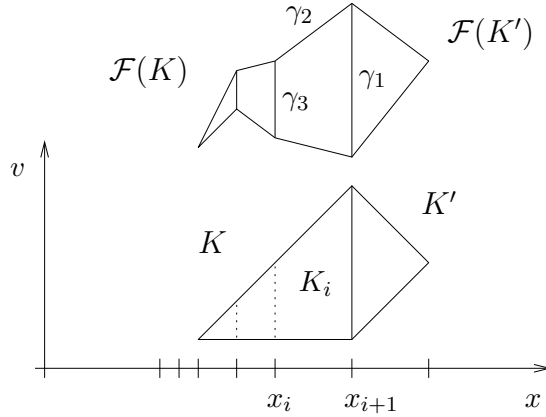


Figure 4: piecewise affine advection.

Proof. In order to study both \mathcal{T}_x and \mathcal{T}_v^n at the same time, we shall consider, for a given interpolation grid $\Gamma \subset \mathbb{R}$ and a function $\tilde{G} \in W^{2,\infty}(\mathbb{R})$, the generic transport operator

$$\mathcal{T} = \mathcal{T}(\Gamma, \tilde{G}) : g \rightarrow g \circ \mathcal{F}^{-1} \quad (4.73)$$

associated to the advection field

$$\mathcal{F} = \mathcal{F}(\Gamma, \tilde{G}) : (x, v) \rightarrow (x, v + G(x)), \quad (4.74)$$

where G is the affine interpolation of \tilde{G} on Γ . Within this context, \mathcal{T}_v^n is obtained by setting $\tilde{G}(x) = \Delta t \tilde{E}^n(x)$ and $\Gamma = \Gamma^n$, while \mathcal{T}_x is obtained by swapping x

and v , and setting $G(x) = \tilde{G}(x) = x\Delta t/2$ for any grid Γ . For sake of simplicity, we shall consider that g is in some $V_{M'}$, with M' a graded mesh (this is in fact the only case we are interested in, but the above estimates hold for any $g \in V$). Denoting then by x_i the points of Γ , we can split each triangle $K \in M'_t$ (where g is affine) into pieces of the form $K_i = K \cap]x_i, x_{i+1}[\times \mathbb{R}$. It is then readily seen that $\mathcal{T}g$ is continuous and affine on each $\mathcal{F}(K_i)$. Let us divide the associated edges into three types: those (like γ_1 in figure 4) which come from a vertical edge of some $K \in M'_t$, those (like γ_2) which come from a non-vertical edge of some K_i , and those (like γ_3) which come from a vertical edge of some K_i but are not of the first type. On each affine piece of $\mathcal{T}g$, we have

$$D(\mathcal{T}g)(x, v) = (\partial_x g - G'(x)\partial_v g, \partial_v g) (\mathcal{F}^{-1}(x, v)) \quad (4.75)$$

so that on any bounded α , we have

$$|\mathcal{T}g|_{W^{1,\infty}(\alpha)} \leq (1 + \|G'\|_{L^\infty}) |g|_{W^{1,\infty}(\mathcal{F}^{-1}(\alpha))}$$

which proves (4.68) and (4.69). Let now γ be an edge associated to $\mathcal{T}g$ such that $\gamma \cap \alpha \neq \emptyset$. If it is a second type edge, we see that the only jump in (4.75) comes from $D(g)$, so that

$$\|[D(\mathcal{T}g)]_\gamma\| \leq (1 + \|G'\|_{L^\infty}) \|[D(g)]_{\mathcal{F}^{-1}(\gamma)}\|, \quad (4.76)$$

and a little geometry also shows that $|\gamma| \leq (1 + \|G'\|_{L^\infty}) |\mathcal{F}^{-1}(\gamma)|$. If γ is a third type edge, the jump in (4.75) now comes from G' , so that

$$\|[D(\mathcal{T}g)]_\gamma\| \leq \|\partial_v g\|_{L^\infty(\mathcal{F}^{-1}(\alpha))} |[G']_{x_i}|, \quad (4.77)$$

where x_i is such that $\gamma \subset \{x_i\} \times \mathbb{R}$, and if finally γ is a first type edge, both $D(g)$ and G' have a jump in (4.75), so that

$$\|[D(\mathcal{T}g)]_\gamma\| \leq (1 + \|G'\|_{L^\infty}) \|[D(g)]_{\mathcal{F}^{-1}(\gamma)}\| + \|\partial_v g\|_{L^\infty(\mathcal{F}^{-1}(\alpha))} |[G']_{x_i}|, \quad (4.78)$$

where x_i is like above. In these two last cases, we clearly have

$$|\gamma| = |\mathcal{F}^{-1}(\gamma)| \leq (1 + \|G'\|_{L^\infty}) |\mathcal{F}^{-1}(\gamma)|.$$

We then denote respectively by α_x and α_v the intervals which are the projections of α on the x and the v -axis: the three different cases gather into

$$\begin{aligned} |\mathcal{T}g|_{\star(\alpha)} &= \sum_{\gamma} |\gamma \cap \alpha| \|[D(\mathcal{T}g)]_\gamma\| \\ &\leq (1 + \|G'\|_{L^\infty})^2 \sum_{\lambda} |\lambda \cap \mathcal{F}^{-1}(\alpha)| \|[D(g)]_\lambda\| \\ &\quad + |\alpha_v| \|\partial_v g\|_{L^\infty(\mathcal{F}^{-1}(\alpha))} \sum_{x_i \in \alpha_x} |[G']_{x_i}|, \end{aligned} \quad (4.79)$$

where the first sum is taken over the edges of $\mathcal{T}g$, and the second one over those of g . In the case where \mathcal{T} is seen as \mathcal{T}_x , G' is the constant $\Delta t/2$ and hence has no jump, so (4.79) reads as (4.70). In order to prove (4.72), we first observe that $|\omega_v| = 2^{-\ell(\alpha)}$. Denoting then by x^- (respectively x^+) the first node of Γ^n lower than $\inf(\alpha_x)$ (respectively greater than $\sup(\alpha_x)$), we infer from condition (4.71) and the graded structure of M that $|x^+ - x^-| \leq 5 \cdot 2^{-\ell(\alpha)}$. It follows that

$$\sum_{x_i \in \alpha_x} |[E^n]_{x_i}| \leq \int_{x^-}^{x^+} |(\tilde{E}^n)''(x)| dx \leq 5 \cdot 2^{-\ell(\alpha)} |\tilde{E}^n|_{W^{2,\infty}},$$

and the lemma is proved. \square

4.4 Properties of the transported meshes

In order to derive interpolation error estimates from the above inequalities, we must verify that condition (4.71) indeed holds when $M = M_2^n$ which is defined by (3.35b). Since this mesh is precisely constructed from \mathcal{F}_v^n , and hence from Γ^n , we need a lemma for that.

Lemma 4.9. *For any graded mesh M , we have*

$$N_x(\mathbb{T}(M, \mathcal{F}_v^n)) \subset N_x(M). \quad (4.80)$$

In other words, the “mesh transport operator” \mathbb{T} associated to some v -directional advection does not enlarge the projection of the meshes on the x -axis.

Proof. To begin with, let us prove that

$$N_x(\tilde{\mathbb{T}}(M, \mathcal{F}_v^n)) \subset N_x(M). \quad (4.81)$$

Given a cell $\alpha \in \tilde{\mathbb{T}}(M, \mathcal{F}_v^n)$, its parent β satisfies by construction $\ell^*(\beta) > \ell(\beta)$, so that there exists a cell $\beta^* \in M$ containing $(\mathcal{F}_v^n)^{-1}(c_\beta)$ such that

$$\ell(\beta^*) = \ell^*(\beta) \geq \ell(\beta) + 1 = \ell(\alpha). \quad (4.82)$$

Considering the one-directional form of \mathcal{F}_v^n , we see that $x_\beta \in \beta_x^*$, and this together with (4.82) yields $\beta_x^* \subset \alpha_x$. Now because of the underlying tree structure that $N_x(M)$ inherits from M , it follows from $\partial(\beta_x^*) \subset N_x(M)$ that $\partial(\alpha_x) \subset N_x(M)$, and (4.81) is proved. Using the fact that $N_x(M)$ also inherits a graded structure from M , we can verify that (4.81) actually implies (4.80), and the lemma is proved. \square

We are now to state a fundamental property of both operators $\mathbb{T}(\cdot, \mathcal{F}_x)$ and $\mathbb{T}(\cdot, \mathcal{F}_v^n)$. For sake of conciseness, we again use the generic advection field (4.74).

Backward influence set. Given a dyadic cell α , we let

$$B(M, \mathcal{F}, \alpha) = \{ \beta \in M, \beta \cap \mathcal{F}^{-1}(\alpha) \neq \emptyset \}$$

be the cells of M that are even partly advected into α .

Lemma 4.10. *Provided the advection field \mathcal{F} satisfies*

$$\|\tilde{G}'\|_{L^\infty} \leq 1/2, \quad (4.83)$$

there is an absolute constant C such that

$$\sup_{\alpha \in \mathbb{T}(M, \mathcal{F})} \#(B(M, \mathcal{F}, \alpha)) \leq C \quad (4.84)$$

for any graded mesh M . In addition, we have

$$\ell(\beta) \leq \ell(\alpha) + 2, \quad \text{for any } \alpha \in \mathbb{T}(M, \mathcal{F}) \text{ and } \beta \in B(M, \mathcal{F}, \alpha). \quad (4.85)$$

The proof is given in the appendix.

Remark 4.11. Applied to \mathcal{F}_x and \mathcal{F}_v^n , the stability condition (4.83) reads

$$\Delta t \leq \min\left(1, (|\tilde{E}^n|_{W^{1,\infty}})^{-1}/2\right),$$

which is not very restrictive. We shall indeed see in section 5 that $|\tilde{E}^n|_{W^{1,\infty}}$ is bounded by some constant which only depends on T , provided that $n\Delta t \leq T$. This actually leads to the stability condition (3.47) in the main theorem, which is *not* a CFL type condition since the restriction on the time step is independent on the space discretization.

The second property of the mesh transport operator is that it does not increase the order of complexity.

Lemma 4.12. *Provided the advection field \mathcal{F} satisfies (4.83), there is an absolute constant C such that*

$$\#(\mathbb{T}(M, \mathcal{F})) \leq C\#(M) \quad (4.86)$$

for any graded mesh M .

The proof is given in the appendix. Combining lemmae 4.8 and 4.10, we now state the practical result that allows us to estimate the interpolation errors on the transported meshes. Recalling that the functionals μ and π are defined in (3.28) and (3.30), we let for any $g \in V \subset W^* \cap W^{1,\infty}$

$$\nu(g, M) := \mu(g, M) + \Delta t \pi(g, M) = \sup_{\alpha \in M} |g|_{W^*(\alpha)} + \Delta t \sup_{\alpha \in M} 2^{-2\ell(\alpha)} |g|_{W^{1,\infty}(\alpha)}.$$

Lemma 4.13 (stability of the transported meshes). *Let us first assume that for any T , the numerical electric field satisfies*

$$|\tilde{E}^n|_{W^{1,\infty}} \leq C_1(T) \quad (4.87)$$

for any n and Δt such that $n\Delta t \leq T$. The transported meshes $M_1^n = \mathbb{T}(M^n, \mathcal{F}_x)$, $M_2^n = \mathbb{T}(M_1^n, \mathcal{F}_v^n)$ and $M^{n+1} = \mathbb{T}(M_3^n, \mathcal{F}_x)$ satisfy then

$$\nu(\mathcal{T}_x f^n, M_1^n) \leq C \nu(f^n, M^n) \quad (4.88)$$

$$\nu(\mathcal{T}_v^n f_1^n, M_2^n) \leq C (1 + |\tilde{E}^n|_{W^{2,\infty}}) \nu(f_1^n, M_1^n) \quad (4.89)$$

$$\nu(\mathcal{T}_x f_3^n, M^{n+1}) \leq C \nu(f_3^n, M_3^n), \quad (4.90)$$

provided that

$$\Delta t \leq \min\left(1, \frac{1}{2C_1(T)}\right). \quad (4.91)$$

Remark 4.14. According to corollary 4.4, we would only need that the transported meshes verify a stability property with respect to the functional μ . Unfortunately, our estimate (4.72) does not exactly implies this, and we therefore need to consider the “relaxed” functional ν for the stability to hold.

Proof. Since condition (4.91) yields

$$\Delta t \max(1/2, |\tilde{E}^n|_{W^{1,\infty}}) \leq 1/2,$$

we have for any $\alpha \in \mathbb{T}(M, \mathcal{F}_x)$

$$\begin{aligned} |\mathcal{T}_x g|_{\star(\alpha)} &\leq 9/4 |g|_{\star(\mathcal{F}_x^{-1}(\alpha))} \leq 9/4 \sum_{\beta \in B(M, \mathcal{F}_x, \alpha)} |g|_{\star(\beta)} \\ &\leq 9/4 \#(B(M, \mathcal{F}_x, \alpha)) \mu(M, g) \leq C \mu(M, g), \end{aligned}$$

where the first inequality is (4.70), the second one follows from the definition of $B(M, \mathcal{F}_x, \alpha)$, the third one from lemma 4.1, and the last one from (4.84). Similarly, we find from (4.68) and (4.85) that

$$\begin{aligned} 2^{-2\ell(\alpha)} |\mathcal{T}_x g|_{W^{1,\infty}(\alpha)} &\leq 3/2 \sup_{\beta \in B(M, \mathcal{F}_x, \alpha)} 2^{-2\ell(\alpha)} |g|_{W^{1,\infty}(\beta)} \\ &\leq 3/2 \sup_{\beta \in B(M, \mathcal{F}_x, \alpha)} 2^{4-2\ell(\beta)} |g|_{W^{1,\infty}(\beta)} \leq C \pi(M, g). \end{aligned}$$

It follows that the x -directional transport satisfies

$$\mu(\mathbb{T}(M, \mathcal{F}_x), \mathcal{T}_x g) \leq C \mu(M, g) \quad \text{and} \quad \pi(\mathbb{T}(M, \mathcal{F}_x), \mathcal{T}_x g) \leq C \pi(M, g),$$

and hence

$$\nu(\mathbb{T}(M, \mathcal{F}_x), \mathcal{T}_x g) \leq C \nu(M, g)$$

which leads to (4.88) and (4.90). Turning to the v -directional transport, we first check from lemma 4.9 that M_2^n satisfies (4.71). We can then apply once more lemmata 4.8 and 4.10, and with similar arguments than above, find that for any cell $\alpha \in M_2^n$,

$$\begin{aligned} |\mathcal{T}_v^n f_1^n|_{\star(\alpha)} &\leq 9/4 |f_1^n|_{\star((\mathcal{F}_v^n)^{-1}(\alpha))} + 5 \cdot 2^{-2\ell(\alpha)} \Delta t |\tilde{E}^n|_{W^{2,\infty}} |f_1^n|_{W^{1,\infty}((\mathcal{F}_v^n)^{-1}(\alpha))} \\ &\leq 9/4 \#(B(M_1^n, \mathcal{F}_v^n, \alpha)) \mu(M_1^n, f_1^n) + C \Delta t |\tilde{E}^n|_{W^{2,\infty}} \pi(M_1^n, f_1^n) \\ &\leq C(1 + |E^n|_{W^{2,\infty}}) [\mu(M_1^n, f_1^n) + \Delta t \pi(M_1^n, f_1^n)]. \end{aligned}$$

We also clearly have

$$\pi(M_2^n, \mathcal{T}_v^n f_1^n) \leq C \pi(M_1^n, f_1^n),$$

and the proof is complete. \square

5 Proof of the error estimate

In section 2.2, smoothness estimates were established for the exact solutions, that allowed us to control the time discretization error. In the same spirit, we now establish some bounds for the numerical solutions, that will next be combined with above lemma 4.13 in order to complete the error analysis. Let us recall that the adaptive scheme reads

$$\begin{aligned} f^{n+1} &:= P_{M^{n+1}} \mathcal{T}_x f_3^n & f_3^n &:= P_{M_2^n} f_2^n \\ f_2^n &:= P_{M_2^n} \mathbb{T}_{n+1} \mathcal{T}_v^n f_1^n & f_1^n &:= P_{M_1^n} \mathcal{T}_x f^n, \end{aligned}$$

and that the associated meshes are either transported, like $M_1^n := \mathbb{T}(M^n, \mathcal{F}_x)$, $M_2^n := \mathbb{T}(M_1^n, \mathcal{F}_v^n)$ and $M^{n+1} := \mathbb{T}(M_3^n, \mathcal{F}_x)$, or adapted like $M_3^n := \mathbb{A}_\varepsilon(f_2^n)$. We let

$$e^n := \|f(t^n) - f^n\|_{L^\infty} \quad (5.92)$$

be the numerical error at the n -th time step.

Maximum principle. Clearly, every operator used in the scheme diminishes the L^∞ norm, so that

$$\|f^{n+1}\|_{L^\infty} \leq \|f_3^n\|_{L^\infty} \leq \cdots \leq \|f^n\|_{L^\infty} \leq \cdots \leq \|f_0\|_{L^\infty}. \quad (5.93)$$

Some orders of magnitude. As a first trivial consequence, we see that the numerical error is uniformly bounded

$$e^n \leq \|f^n\|_{L^\infty} + \|f(t^n)\|_{L^\infty} \leq 2\|f_0\|_{L^\infty}. \quad (5.94)$$

Condition (3.47) implies $\varepsilon \leq \Delta t \leq 1$, and since the interpolation errors estimates are about ε , we can also assume that $\varepsilon \leq e^n$ (more precisely, replacing e^n by $\max(e^n, \varepsilon)$ in the sequel will not change the results), so that we shall use

$$\varepsilon \leq \min(\Delta t, e^n) \leq \max(\Delta t, e^n) \leq C \quad (5.95)$$

where C only depends on f_0 .

Support control. We recall that the soft truncation operator \mathbb{T}_n has been defined in (3.42) to control the support in the v direction. In particular, for a given mesh M and density g , we only have $\Sigma_v(P_M g) \leq \Sigma_v(g) + 2^{-\ell_0}$, while

$$\Sigma_v(\mathbb{T}_n g) \leq \hat{Q}_n + 2^{-\ell_0} \leq Q_n + 3 \cdot 2^{-\ell_0}. \quad (5.96)$$

It follows that for any n , we have

$$\begin{aligned} \Sigma_v(f^{n+1}) &\leq \Sigma_v(\mathcal{T}_x f_3^n) + 2^{-\ell_0} \leq \Sigma_v(f_3^n) + 2^{-\ell_0} \leq \Sigma_v(f_2^n) + 2 \cdot 2^{-\ell_0} \\ &\leq \Sigma_v(\mathbb{T}_{n+1} \mathcal{T}_v^n f_1^n) + 3 \cdot 2^{-\ell_0} \leq Q_{n+1} + 6 \cdot 2^{-\ell_0} \end{aligned}$$

and

$$\Sigma_v(f_1^n) \leq \Sigma_v(\mathcal{T}_x f^n) + 2^{-\ell_0} \leq \Sigma_v(f^n) + 2^{-\ell_0} \leq Q_n + 7 \cdot 2^{-\ell_0} \leq \tilde{\Sigma}_v \quad (5.97)$$

(we recall that $\tilde{\Sigma}_v := Q(0) + 2T + 7 \cdot 2^{-\ell_0}$).

Bounds for the numerical electric field (part one). Equipped with (5.93) and (5.97), we have a first estimate for the numerical electric field. Namely, we see from (2.23) that

$$|\tilde{E}(f_1^n)|_{W^{1,\infty}} = \left\| \int f_1^n(\cdot, v) dv - 1 \right\|_{L^\infty} \leq \Sigma_v(f_1^n) \|f_1^n\|_{L^\infty} + 1 \leq \tilde{\Sigma}_v \|f_0\|_{L^\infty} + 1,$$

and from (3.36), that

$$|\tilde{E}^n|_{W^{1,\infty}} \leq 2|\tilde{E}(f_1^n)|_{W^{1,\infty}} \leq 2(\tilde{\Sigma}_v \|f_0\|_{L^\infty} + 1). \quad (5.98)$$

Together with condition (3.47) imposed on Δt , this estimate allows us to apply lemma 4.13.

Interpolation error estimates (part one). According then to lemmae 4.13 and 4.7, we have for any n

$$\begin{aligned}
\mu(\mathcal{T}_x f^n, M_1^n) &\leq \nu(\mathcal{T}_x f^n, M_1^n) = \nu(\mathcal{T}_x f^n, \mathbb{T}(M^n, \mathcal{F}_x)) \\
&\leq C \nu(f^n, M^n) = C \nu(P_{M^n} \mathcal{T}_x f_3^{n-1}, M^n) \\
&\leq C \nu(\mathcal{T}_x f_3^{n-1}, M^n) = C \nu(\mathcal{T}_x f_3^{n-1}, \mathbb{T}(M_3^{n-1}, \mathcal{F}_x)) \\
&\leq C \nu(f_3^{n-1}, M_3^{n-1}) = C \nu(P_{M_3^{n-1}} f_2^{n-1}, M_3^{n-1}) \\
&\leq C \nu(f_2^{n-1}, M_3^{n-1}) = C \nu(f_2^{n-1}, \mathbb{A}_\varepsilon(f_2^{n-1})) \\
&\leq C \varepsilon,
\end{aligned} \tag{5.99}$$

where this last inequality follows from the property (3.31) of the mesh adaptation operator \mathbb{A}_ε . We emphasize that no induction argument was used, so that no constant appearing in the above computation depend on n . Using then corollary 4.4, we find

$$\|(I - P_{M_1^n}) \mathcal{T}_x f^n\|_{L^\infty} \leq C \varepsilon \tag{5.100}$$

and since (5.99) holds for any n , we also have

$$\|(I - P_{M_3^n}) f_2^n\|_{L^\infty} \leq C \varepsilon \tag{5.101}$$

and

$$\|(I - P_{M^{n+1}}) \mathcal{T}_x f_3^n\|_{L^\infty} \leq C \varepsilon. \tag{5.102}$$

Estimating the lack of conservativity. We recall that one of the basic properties of the Vlasov equation is that for any t , the mass of the exact solution is constant and according to (2.8), equal to $\|f(t)\|_{L^1} = 1$. This is not the case with the numerical solutions (remember that the interpolations are not conservative), but we have

$$\begin{aligned}
\left| \|f_1^n\|_{L^1} - 1 \right| &\leq \|f_1^n - \mathcal{T}_x f^n\|_{L^1} + \|\mathcal{T}_x(f^n - f(t^n))\|_{L^1} + \|\mathcal{T}_x f(t^n)\|_{L^1} - 1 \\
&\leq \|(I - P_{M_1^n}) \mathcal{T}_x f^n\|_{L^1} + \|f^n - f(t^n)\|_{L^1} + \|f(t^n)\|_{L^1} - 1 \\
&\leq \tilde{\Sigma}_v \left[\|(I - P_{M_1^n}) \mathcal{T}_x f^n\|_{L^\infty} + \|f^n - f(t^n)\|_{L^\infty} \right] \\
&\leq \tilde{\Sigma}_v (\varepsilon + e^n) \leq 2\tilde{\Sigma}_v e^n
\end{aligned} \tag{5.103}$$

where the second inequality comes from the conservativity of \mathcal{T}_x , and in the third one we use that the support of every involved functions as a volume bounded by $\tilde{\Sigma}_v$, and also that $\|f(t^n)\|_{L^1}$ is precisely 1. The two last inequalities follow from (5.100) and (5.95), respectively.

Bounds for the numerical electric field (part two). Turning again to the electric field, we see from (2.23) and the above estimate (5.103) that

$$\|\tilde{E}(f_1^n)\|_{L^\infty} \leq \|f_1^n\|_{L^1} + 1 \leq 2 + 2\tilde{\Sigma}_v e^n.$$

In addition, we have

$$\left| \tilde{E}^n(1) - \tilde{E}^n(0) \right| = \left| \int \tilde{E}(f_1^n)'(x) dx \right| = \left| \iint f_1^n(x, v) dx dv - 1 \right| \leq 2\tilde{\Sigma}_v e^n, \tag{5.104}$$

so that the definition of E^n yields

$$\|E^n\|_{L^\infty} \leq \|\tilde{E}^n\|_{L^\infty} \leq \|\tilde{E}(f_1^n)\|_{L^\infty} + \left| \tilde{E}^n(1) - \tilde{E}^n(0) \right| \leq 2 + 4\tilde{\Sigma}_v e^n. \quad (5.105)$$

We will also need the following estimates in the sequel: in the first place, we have from (2.23)

$$\|\tilde{E}(\mathcal{T}_x f(t^n)) - \tilde{E}(f_1^n)\|_{L^\infty} \leq \|\mathcal{T}_x f(t^n) - f_1^n\|_{L^1} \leq C(T) e^n, \quad (5.106)$$

where the second inequality follows from the estimates in (5.103). In the second place, (3.36) and (5.104) also give

$$\|\tilde{E}(f_1^n) - \tilde{E}^n\|_{L^\infty} \leq C(T) e^n, \quad (5.107)$$

and in the third place, we can bound the interpolation error of E^n by

$$\|\tilde{E}^n - E^n\|_{L^\infty} \leq \frac{1}{8} \sup_i |x_{i+1} - x_i|^2 \|(\tilde{E}^n)''\|_{L^\infty([x_i, x_{i+1}])}$$

where the x_i denote the points of the interpolation grid Γ^n . We have

$$\|(\tilde{E}^n)''\|_{L^\infty([x_i, x_{i+1}])} = \left\| \int \partial_x f_1^n(\cdot, v) dv \right\|_{L^\infty([x_i, x_{i+1}])} \leq \Sigma_v(f_1^n) \sup_\alpha |f_1^n|_{W^{1,\infty}(\alpha)}$$

the sup being taken over all the cells $\alpha \in M_1^n$ such that $\alpha_x \cap [x_i, x_{i+1}] \neq \emptyset$. According to the construction of Γ^n , any such cell satisfies $|x_{i+1} - x_i| \leq 2^{-\ell(\alpha)}$, so that using the uniform bound on the numerical support (5.97), we compute

$$\|\tilde{E}^n - E^n\|_{L^\infty} \leq C(T) \pi(f_1^n, M_1^n) \leq C(T) \varepsilon, \quad (5.108)$$

since it is seen from lemma 4.7 and inequality (5.99) that

$$\nu(f_1^n, M_1^n) \leq C \varepsilon. \quad (5.109)$$

The outer error. We are now able to give an estimate for the *outer error*

$$e_{\text{out}}^n := \|f(t^n) - f^n\|_{L^\infty((\hat{\Omega}_n)^c)}$$

(we recall that $\hat{\Omega}_n$ was defined together with Ω_n in remark 3.5). Using that $f(t^{n+1})$ vanishes outside $\hat{\Omega}_{n+1}$, we have

$$\begin{aligned} e_{\text{out}}^{n+1} &= \|f^{n+1}\|_{L^\infty((\hat{\Omega}_{n+1})^c)} \leq \|\mathcal{T}_x f_3^n\|_{L^\infty((\hat{\Omega}_{n+1})^c)} \leq \|f_3^n\|_{L^\infty((\hat{\Omega}_{n+1})^c)} \\ &\leq \|f_2^n\|_{L^\infty((\hat{\Omega}_{n+1})^c)} \leq \|\mathbb{T}_{n+1} \mathcal{T}_v f_1^n\|_{L^\infty((\hat{\Omega}_{n+1})^c)} \leq \|\mathcal{T}_v f_1^n\|_{L^\infty((\hat{\Omega}_{n+1})^c)}, \end{aligned}$$

where the first, second and fourth inequalities follow from the diminishing property (3.44) of the interpolations on the set $(\hat{\Omega}_{n+1})^c$. The third (resp. the last) inequality follows from the fact that \mathcal{T}_x (resp. \mathbb{T}_{n+1}) diminishes the L^∞ norm on $(\hat{\Omega}_{n+1})^c$. We then observe that since any (x, v) outside $\hat{\Omega}_{n+1}$ satisfies $|v| \leq \hat{Q}_{n+1}$, we observe using (3.41) and (5.105) that

$$|v - \Delta t E^n(x)| \geq \hat{Q}_{n+1} - \Delta t \|E^n\|_{L^\infty} \geq Q_n + 2^{-\ell_0} - 4\Delta t \tilde{\Sigma}_v e^n \geq Q_n,$$

where this last inequality follows from (3.47). This means that $\mathcal{F}_v^n(\Omega_n) \subset \hat{\Omega}_{n+1}$, and this is what motivated the choice of \hat{Q}_n . We find then

$$\begin{aligned} \|\mathcal{T}_v^n f_1^n\|_{L^\infty((\hat{\Omega}_{n+1})^c)} &\leq \|f_1^n\|_{L^\infty((\Omega_n)^c)} \\ &\leq \|\mathcal{T}_x f^n\|_{L^\infty((\Omega_n)^c)} + \|(I - P_{M_1^n})\mathcal{T}_x f^n\|_{L^\infty} \\ &\leq \|f^n\|_{L^\infty((\Omega_n)^c)} + C\varepsilon \leq e^n + C\varepsilon. \end{aligned} \quad (5.110)$$

Here the third inequality is (5.100), and the last one again follows from the fact that $f(t^n)$ vanishes outside Ω_n . We therefore have the following estimate for the outer error:

$$e_{\text{out}}^{n+1} \leq e^n + C\varepsilon. \quad (5.111)$$

Lipschitz bound. According to the definition (3.42) of the soft truncation operator, we have

$$\begin{aligned} \|\partial_v \mathbb{T}_{n+1} \mathcal{T}_v^n f_1^n\|_{L^\infty} &\leq \max\left(\|\partial_v \mathcal{T}_v^n f_1^n\|_{L^\infty}, 2^{\ell_0} \|\mathcal{T}_v^n f_1^n\|_{L^\infty((\hat{\Omega}_{n+1})^c)}\right) \\ &\leq \|\partial_v \mathcal{T}_v^n f_1^n\|_{L^\infty} + 2^{\ell_0} \|\mathcal{T}_v^n f_1^n\|_{L^\infty((\hat{\Omega}_{n+1})^c)} \\ &\leq \|\partial_v f_1^n\|_{L^\infty} + C(T) e^n, \end{aligned}$$

where this last inequality follows from $\|\partial_v \mathcal{T}_v^n f_1^n\|_{L^\infty} = \|\partial_v f_1^n\|_{L^\infty}$ the above estimate (5.110) and (5.95). Because \mathbb{T}_{n+1} diminishes the $\|\partial_x \cdot\|_{L^\infty}$ semi-norm, we have on the other hand

$$\|\partial_x \mathbb{T}_{n+1} \mathcal{T}_v^n f_1^n\|_{L^\infty} \leq \|\partial_x \mathcal{T}_v^n f_1^n\|_{L^\infty} \leq \|\partial_x f_1^n\|_{L^\infty} + \Delta t |\tilde{E}^n|_{W^{1,\infty}} \|\partial_v f_1^n\|_{L^\infty}.$$

The uniform Lipschitz bound (5.98) for \tilde{E}^n yields then

$$\begin{aligned} |\mathbb{T}_{n+1} \mathcal{T}_v^n f_1^n|_{W^{1,\infty}} &= \|\partial_x \mathbb{T}_{n+1} \mathcal{T}_v^n f_1^n\|_{L^\infty} + \|\partial_v \mathbb{T}_{n+1} \mathcal{T}_v^n f_1^n\|_{L^\infty} \\ &\leq |f_1^n|_{W^{1,\infty}} [1 + C(T)\Delta t] + C(T) e^n. \end{aligned} \quad (5.112)$$

According to the Lipschitz diminishing property (4.64) of the interpolations together with estimate (4.68), we finally have

$$\begin{aligned} |f^{n+1}|_{W^{1,\infty}} &\leq |\mathcal{T}_x f_3^n|_{W^{1,\infty}} \leq (1 + \Delta t/2) |f_3^n|_{W^{1,\infty}} \\ &\leq (1 + \Delta t/2) |f_2^n|_{W^{1,\infty}} \leq (1 + \Delta t/2) |\mathbb{T}_{n+1} \mathcal{T}_v^n f_1^n|_{W^{1,\infty}} \\ &\leq (1 + \Delta t/2)(1 + C(T)\Delta t) |f_1^n|_{W^{1,\infty}} + C(T) e^n \\ &\leq (1 + C(T)\Delta t) |\mathcal{T}_x f^n|_{W^{1,\infty}} + C(T) e^n \\ &\leq (1 + C(T)\Delta t) |f^n|_{W^{1,\infty}} + C(T) e^n. \end{aligned} \quad (5.113)$$

Bounds for the numerical electric field (part three). Using again (2.23) and (3.36), we see that

$$|\tilde{E}^n|_{W^{2,\infty}} = |\tilde{E}(f_1^n)|_{W^{2,\infty}} = \left\| \int \partial_x f_1^n(\cdot, v) dv \right\|_{L^\infty} \leq \Sigma_v(f_1^n) |f_1^n|_{W^{1,\infty}},$$

and it follows from the inside inequalities of (5.113) that

$$|\tilde{E}^n|_{W^{2,\infty}} \leq C(T) (|f^n|_{W^{1,\infty}} + e^n). \quad (5.114)$$

Interpolation error estimates (part two). Using (5.109) and (4.89), this last estimate allows us to bound the last interpolation error by

$$\begin{aligned} \|(I - P_{M_2^n})\mathcal{T}_v^n f_1^n\|_{L^\infty} &\leq \nu(\mathcal{T}_v^n f_1^n, M_2^n) \\ &\leq C(1 + |\tilde{E}^n|_{W^{2,\infty}})\nu(f_1^n, M_1^n) \\ &\leq C(T)(1 + |f^n|_{W^{1,\infty}})\varepsilon. \end{aligned} \quad (5.115)$$

The inside error. Equipped with the a priori bounds for the interpolation errors (5.100) - (5.102) and (5.115), we now focus on

$$e_{\text{in}}^n := \|f(t^n) - f^n\|_{L^\infty(\hat{\Omega}_n)}. \quad (5.116)$$

First of all, we observe from (3.45) that \mathcal{T}_{n+1} does not appear in the restriction of f^{n+1} to $\hat{\Omega}_{n+1}$:

$$(f^{n+1})|_{\hat{\Omega}_{n+1}} = (P_{M^{n+1}}\mathcal{T}_x P_{M_2^n} P_{M_2^n} \mathcal{T}_v^n P_{M_1^n} \mathcal{T}_x f^n)|_{\hat{\Omega}_{n+1}}. \quad (5.117)$$

As announced in section 3.4, we write the inside error term (5.116) as the sum of three error terms: (i) the time discretization error

$$\mathcal{E}_t^{n+1} := \|f(t^{n+1}) - \mathbb{S}_{\Delta t} f(t^n)\|_{L^\infty} \leq C(T)\Delta t^3 \quad (5.118)$$

which can be estimated on the entire domain Ω using lemma 2.4, (ii) a space discretization error

$$\mathcal{E}_s^{n+1} := \|(\mathcal{T}_x \mathcal{T}_v^n \mathcal{T}_x - \mathbb{S}_{\Delta t, \varepsilon})f^n\|_{L^\infty(\hat{\Omega}_{n+1})}$$

which slightly differs from what was proposed in section 3.4 but is more relevant to our aims, and (iii) an additional ‘‘coupling term’’

$$\mathcal{E}_c^{n+1} := \|\mathcal{T}_x \mathcal{T}_v \mathcal{T}_x f(t^n) - \mathcal{T}_x \mathcal{T}_v^n \mathcal{T}_x f^n\|_{L^\infty(\hat{\Omega}_{n+1})}.$$

We thus have

$$e_{\text{in}}^{n+1} \leq \mathcal{E}_t^{n+1} + \mathcal{E}_s^{n+1} + \mathcal{E}_c^{n+1}. \quad (5.119)$$

According to (5.117), we decompose

$$\begin{aligned} \mathcal{E}_s^{n+1} &\leq \|\mathcal{T}_x \mathcal{T}_v^n (I - P_{M_1^n}) \mathcal{T}_x f^n\|_{L^\infty} + \|\mathcal{T}_x (I - P_{M_2^n}) \mathcal{T}_v^n f_1^n\|_{L^\infty} \\ &\quad + \|\mathcal{T}_x (I - P_{M_3^n}) f_2^n\|_{L^\infty} + \|(I - P_{M^{n+1}}) \mathcal{T}_x f_3^n\|_{L^\infty} \\ &\leq C(1 + |f^n|_{W^{1,\infty}})\varepsilon, \end{aligned} \quad (5.120)$$

the second inequality following from estimates (5.100) - (5.102) and (5.115). Turning to the coupling error, we then observe from the linearity of \mathcal{T}_x and \mathcal{T}_v^n that

$$\mathcal{E}_c^{n+1} \leq \|\mathcal{T}_x \mathcal{T}_v^n \mathcal{T}_x (f(t^n) - f^n)\|_{L^\infty} + \|\mathcal{T}_x (\mathcal{T}_v - \mathcal{T}_v^n) \mathcal{T}_x f(t^n)\|_{L^\infty},$$

whereas the definition of \mathcal{T}_v and \mathcal{T}_v^n yields

$$\|(\mathcal{T}_v - \mathcal{T}_v^n) \mathcal{T}_x f(t^n)\|_{L^\infty} \leq \Delta t \|\tilde{E}(\mathcal{T}_x f(t^n)) - E^n\|_{L^\infty} |\mathcal{T}_x f(t^n)|_{W^{1,\infty}}.$$

Using then (5.106) - (5.108), we have $\|\tilde{E}(\mathcal{T}_x f(t^n)) - E^n\|_{L^\infty} \leq C(T)(e^n + \varepsilon)$, while (4.68), (5.95) and (2.15) give $|\mathcal{T}_x f(t^n)|_{W^{1,\infty}} \leq C|f(t^n)|_{W^{1,\infty}} \leq C(T)$. Gathering these estimates, we see that

$$\mathcal{E}_c^{n+1} \leq e^n(1 + C(T)\Delta t), \quad (5.121)$$

which together with (5.118)-(5.120) yields

$$e_{\text{in}}^{n+1} \leq e^n(1 + C(T)\Delta t) + C(T)[\Delta t^3 + \varepsilon(1 + |f^n|_{W^{1,\infty}})]$$

(the constants also depending on the initial solution f_0).

End of the proof. From the a priori estimates of both outer (5.111) and inside errors (above), we find

$$e^{n+1} \leq e^n(1 + C(T)\Delta t) + C(T)[\Delta t^3 + \varepsilon(1 + |f^n|_{W^{1,\infty}})] \quad (5.122)$$

and we may also recall (5.113):

$$|f^{n+1}|_{W^{1,\infty}} \leq |f^n|_{W^{1,\infty}}(1 + C(T)\Delta t) + C(T)\Delta t e^n. \quad (5.123)$$

Because assumption (3.47) implies $\varepsilon \leq \Delta t^2$, a first Gronwall argument applied to $e^{n+1} + \Delta t|f^{n+1}|_{W^{1,\infty}}$ yields $\sup_{n \leq N}(e^n + \Delta t|f^n|_{W^{1,\infty}}) \leq C(T)\Delta t$. It follows that $|f^n|_{W^{1,\infty}}$ is uniformly bounded, so that we can apply a second Gronwall argument to (5.122) and find estimate (3.46), which ends the proof. \square

6 Numerical results

We tested our scheme with the classical semi-gaussian beam simulation, which is known to develop thin structures in the phase space. Because the usual initial semi-gaussian data $f_{\text{sg}} := a \exp(-(v/b)^2) \mathbb{1}_{[-c,c] \times \mathbb{R}}$ is neither continuous, nor has a bounded support, we replaced it with

$$f_0 := a \exp(-(v/b)^2) \rho(x, v) \simeq f_{\text{sg}},$$

where ρ is a compactly supported $W^{2,\infty}$ approximation of $\mathbb{1}_{[-c,c] \times \mathbb{R}}$. We set $a = 5.794$, $b = 0.122$ and $c = 0.172$. We also classically added an affine external electric field $E_{\text{ext}}(x)$ to prevent the plasma from dispersing too much. We present below a few results given by both adaptive and uniform schemes: according to the balancing of the main error estimates, we let $h = \Delta t^{3/2}$ for the uniform solutions $f_{u,h}^n$ and $\varepsilon = c\Delta t^3$ for the adaptive ones (with $c = 320$). For practical reasons, we imposed the constraint that the levels of the cells never exceed a prescribed $L = 10$. Since the exact solution f is unknown, the accuracy of the solutions has been evaluated using the uniform solution $f_L := f_{h(L)}$ computed with the finest space step $h(L) := 2^L = 1/1024$ (because of the practical constraint on the level of the cells, we may notice that f_L is also given by the adaptive scheme when $\varepsilon = 0$). We should also mention that the scheme implemented at the present stage differs in some points with the one described in this article. In particular, the advection scheme does not follow in practice the time splitting scheme $\mathbb{S}_{\Delta t}$ but rather uses a single transport operator in the (x, v) space. Nevertheless, we believe that since the key feature of our scheme is its mesh evolution strategy, these changes only have a small effect on the numerical results.

Lack of conservativity. Because the scheme is not conservative, it was interesting to see how well (or how bad) the mass of the solutions is preserved in practice (from inequality (5.103), we know that this is related to the numerical accuracy). On figure 5, the evolution of the global mass ratio $\|f^N\|_{L^1}/\|f_L^0\|_{L^1}$ is plotted against $T = N\Delta t$ for different values of Δt (left), and against the size N of the associated meshes for both adaptive and uniform solutions (right). In both cases we observe that the lack of conservativity tends to zero as the size of the meshes increases.

Numerical accuracy. On figure 6, the distance between f^N and the “approached exact solution” f_L^N is plotted in log-log scale against Δt . Distances are drawn in L^∞ (left) and L^1, L^2 (right) in order to verify that our strategy also achieves nice convergence rates in these metrics. The computed least square slopes are slightly better than expected from estimate (3.46).

Optimal complexity. In order to appraise the relevance of section 3.5, and in particular estimate (3.51), we represented on figure 7 the L^∞ error against the computational time (left) and the size of the meshes (right) for several executions of both adaptive and uniform schemes. Here the decision to replace the exact

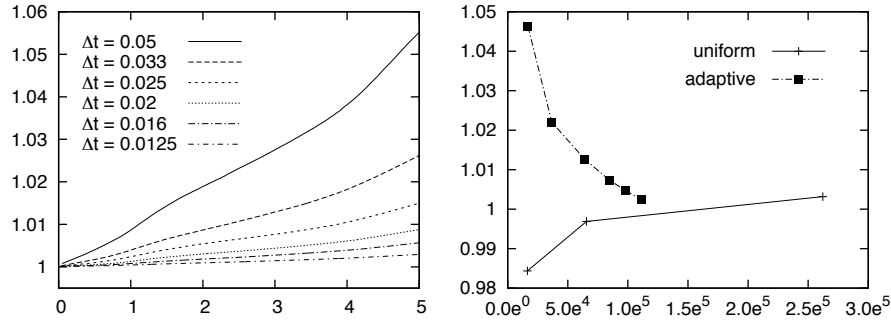


Figure 5: mass ratio vs. time T for adaptive solutions (left) and vs. mesh cardinality N for both uniform and adaptive solutions at $T = 4.5$ (right).

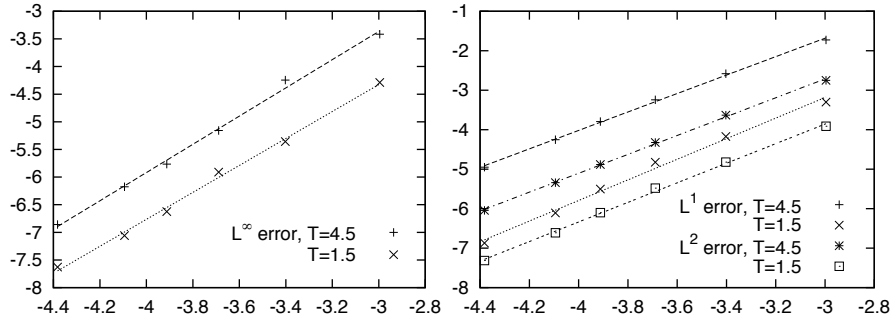


Figure 6: convergence rates. Error between f^N and f_L^N in L^∞ (left) and L^1, L^2 metrics (right) vs. Δt in log-log scale for $T = 1.5$ (slopes are 2.44, 2.61 and 2.48 resp.) and $T = 4.5$ (slopes are 2.55, 2.33 and 2.33 resp.).

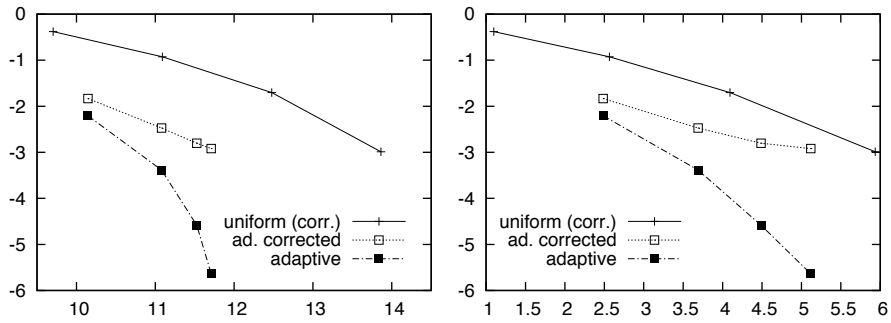


Figure 7: L^∞ errors vs. mesh cardinality N (left) and cpu time in minutes (right) in log-log scale for both adaptive and uniform solutions.

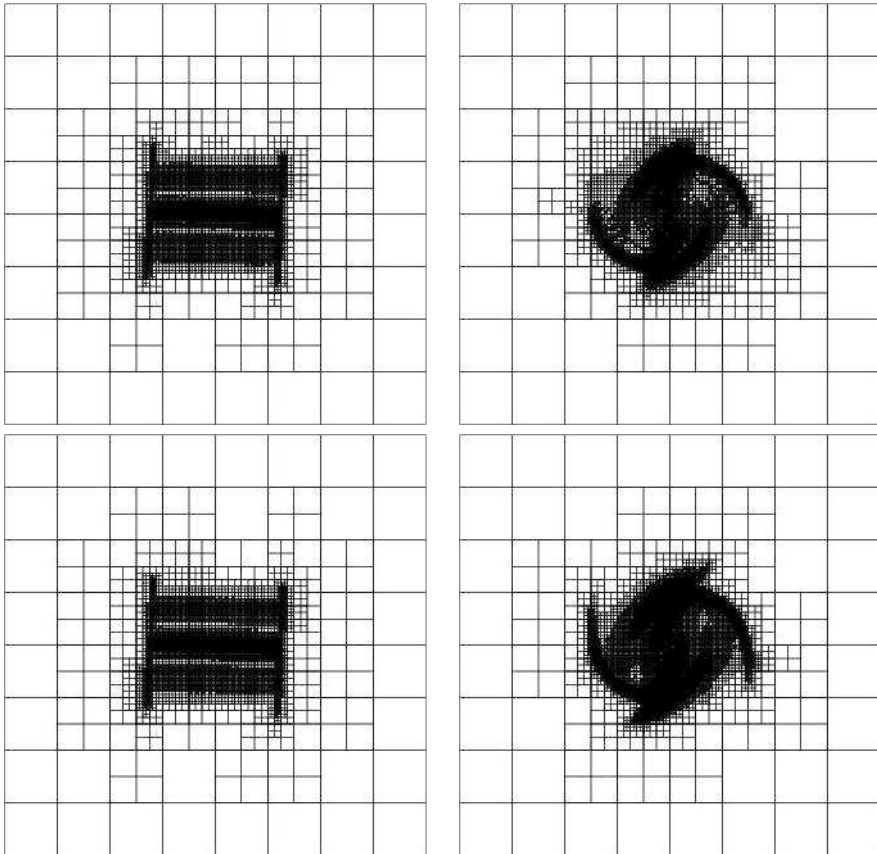


Figure 8: comparison of the meshes resulting from the adaptive scheme (up) and from the compression \mathbb{A}_ε of the finest uniform solution (below), at $T = 0.05$ (left) and $T = 10.05$ (right).

$f(T)$ with f_L^N computed on the finest uniform mesh of level L must be discussed: it indeed overstates the accuracy of the adaptive solutions f^N that are very close to f_L^N . Next to the black boxes that represent the distance $\tilde{e}^N = \|f^N - f_L^N\|_{L^\infty}$,

we therefore plotted in white boxes the *corrected* quantities $\tilde{e}^N + \tilde{e}$, where \tilde{e} is a reasonable estimate for $\|f_L^N - f(T)\|_{L^\infty}$ obtained as follows: because the errors $\|f_{h(\ell)}^N - f(T)\|_{L^\infty}$ resulting from the uniform scheme decay geometrically with ℓ , they are of the same order than the approached ones $\|f_{h(\ell)}^N - f_L^N\|_{L^\infty}$ when $\ell \leq L - 1$, so that we find \tilde{e} by extrapolating those “coarse grids” approached errors. This in turn bounds the accuracy of the adaptive solutions by above, *but by prohibiting it to do better than f_L , it also gives a pessimistic idea of the adaptive schemes performances*, especially when measuring the computational time. Anyhow, the resulting “corrected error vs. cardinality” curves decay with a slope of about -0.7 in log-log scale, which confirms estimates (3.48) and (3.51). Concerning the savings, we also see that for a given accuracy, the uniform meshes are about 100 times as big as the adaptive ones. This ratio is unfortunately not achieved when considering the cpu times, which is mainly due to the fact that the adaptive method dynamically manages tree structured meshes and has therefore many overheads compared to the uniform one. For instance, the cpu time ratio corresponding to a “corrected error” of $0.084 \simeq e^{-2.47}$ is only of 4.5. This rather disappointing observation should nevertheless be moderated by the fact that we certainly did not implement our scheme in an optimal way, and by the fact that we imposed a maximal level constraint on the cells. We finally represented on figure 8 the meshes M^N given by the adaptive scheme (when $\Delta t = 0.05$ and ε as above) together with those $\mathbb{A}_\varepsilon(f_L^N)$ obtained by “compressing” our best uniform solution f_L . *This shows that our strategy generates meshes which are very close to the optimal ones.*

7 Appendix

7.1 Proof of lemma 2.4

Let (x, v) be fixed in \mathbb{R}^2 . Since f is constant along the characteristics, we have

$$f(t^{n+1}, x, v) = f(t^n, X(t^n), V(t^n))$$

where $(X, V)(s) = (X, V)(s; t^{n+1}, x, v)$ is the integral curve solution of (1.4) that satisfies $(X, V)(t^{n+1}) = (x, v)$. On the other hand, denoting by X^n and V^n the feet of the numerical characteristics $\tilde{X}(t^n; t^{n+1}, x, v)$ and $\tilde{V}(t^n; t^{n+1}, x, v)$ defined in (2.27), we have $\mathbb{S}_{\Delta t} f(t^n)(x, v) = f(t^n, X^n, V^n)$. According to lemma 2.3, $f(t^n)$ is Lipschitz as soon as f_0 is, and

$$\begin{aligned} \|f(t^{n+1}) - \mathcal{S}f(t^n)\|_{L^\infty(\Omega)} &\leq |f(t^n)|_{W^{1,\infty}(\Omega)} (|X(t^n) - X^n| + |V(t^n) - V^n|) \\ &\leq C(T) \max(|X(t^n) - X^n|, |V(t^n) - V^n|), \end{aligned}$$

so that we are left to prove

$$\max(|X^n - X(t^n)|, |V^n - V(t^n)|) \leq C(T)\Delta t^3. \quad (7.124)$$

Denoting $E_X(t) := E(t, X(t))$ the exact field along the characteristic curve, we use again lemma 2.3 together with the characteristic equation (1.4) to bound the following time derivatives (for concise notations, the $\|\cdot\|_\infty$ norm here denotes $\|\cdot\|_{L^\infty([0,T], L^\infty([0,1]))}$)

$$\|E_X\|_{L^\infty([0,T])} \leq C(T) \quad (7.125)$$

$$\begin{aligned}\|\dot{E}_X\|_{L^\infty([0,T])} &\leq \|\partial_t E\|_\infty + \|V\|_{L^\infty([0,T])}\|\partial_x E\|_\infty \\ &\leq \|\partial_t E\|_\infty + Q(T)\|\partial_x E\|_\infty \leq C(T)\end{aligned}\quad (7.126)$$

$$\begin{aligned}\|\ddot{E}_X\|_{L^\infty([0,T])} &\leq \|\partial_{tt}^2 E\|_\infty + 2\|V\|_{L^\infty([0,T])}\|\partial_{tx}^2 E\|_\infty \\ &\quad + \|V^2\|_{L^\infty([0,T])}\|\partial_{xx}^2 E\|_\infty + \|E\|_\infty\|\partial_x E\|_\infty \leq C(T).\end{aligned}\quad (7.127)$$

We decompose then

$$\begin{aligned}X^n - X(t^n) &= X(t^{n+1}) - X(t^n) - v\Delta t + \Delta t^2/2 \tilde{E}(\mathcal{T}_x f(t^n))(x - v\Delta t/2) \\ &= \mathcal{E}_1 + \frac{\Delta t^2}{2}(\mathcal{E}_2 + \mathcal{E}_3),\end{aligned}$$

with

$$\begin{aligned}\mathcal{E}_1 &:= X(t^{n+1}) - X(t^n) - v\Delta t + \Delta t^2/2 E_X(t^{n+1/2}) \\ \mathcal{E}_2 &:= E(t^{n+1/2}, x - v\Delta t/2) - E_X(t^{n+1/2}) \\ \mathcal{E}_3 &:= \tilde{E}(\mathcal{T}_x f(t^n))(x - v\Delta t/2) - E(t^{n+1/2}, x - v\Delta t/2)\end{aligned}$$

and $t^{n+1/2} = (n + 1/2)\Delta t$. Similarly,

$$\begin{aligned}V^n - V(t^n) &= V(t^{n+1}) - V(t^n) - \Delta t \tilde{E}(\mathcal{T}_x f(t^n))(x - v\Delta t/2) \\ &= \mathcal{E}_4 + \Delta t(\mathcal{E}_2 + \mathcal{E}_3)\end{aligned}$$

with

$$\mathcal{E}_4 := V(t^{n+1}) - V(t^n) - \Delta t E_X(t^{n+1/2}).$$

It remains then to prove

$$|\mathcal{E}_1| \leq C(T)\Delta t^3, \quad |\mathcal{E}_2| \leq C(T)\Delta t^2, \quad |\mathcal{E}_3| \leq C(T)\Delta t^2 \quad \text{and} \quad |\mathcal{E}_4| \leq C(T)\Delta t^3.$$

For the first term, we have

$$\begin{aligned}\mathcal{E}_1 &= \int_{t^n}^{t^{n+1}} (V(t) - v) dt + \Delta t^2/2 E_X(t^{n+1/2}) \\ &= \int_{t^n}^{t^{n+1}} (V(t) - V(t^{n+1})) dt - \int_{t^n}^{t^{n+1}} \text{int}_t^{t^{n+1}} E_X(t^{n+1/2}) ds dt \\ &= \int_{t^n}^{t^{n+1}} \text{int}_t^{t^{n+1}} (E_X(t^{n+1/2}) - E_X(s)) ds dt.\end{aligned}$$

From (7.126), we see that

$$|E_X(t^{n+1/2}) - E_X(s)| \leq |\dot{E}_X|_{L^\infty([0,T])}|t^{n+1/2} - s| \leq C(T)\Delta t,$$

which yields $|\mathcal{E}_1| \leq C(T)\Delta t^3$. For the second term, we write

$$\begin{aligned}|\mathcal{E}_2| &= |E(t^{n+1/2}, x - v\Delta t/2) - E(t^{n+1/2}, X(t^{n+1/2}))| \\ &\leq \|\partial_x E(t^{n+1/2})\|_{L^\infty([0,1])}|X(t^{n+1/2}) - x + v\Delta t/2| \\ &\leq C(T)|X(t^{n+1/2}) - X(t^{n+1}) + v\Delta t/2| \\ &\leq C(T) \int_{t^{n+1/2}}^{t^{n+1}} |v - V(t)| dt \\ &\leq C(T) \int_{t^{n+1/2}}^{t^{n+1}} |V(t^{n+1}) - V(t)| dt \\ &\leq C(T)\|E_X\|_{L^\infty([0,T])}\Delta t^2 \leq C(T)\Delta t^2\end{aligned}$$

where this last inequality comes from (7.125). Considering then the third term, we have from (2.10) and (2.23)

$$\begin{aligned}
|\mathcal{E}_3| &= \left| \int K(x - v\Delta t/2, y) \int [f(t^n, y - v\Delta t/2, v) - f(t^{n+1/2}, y, v)] dv dy \right| \\
&\leq \int \left| \int [f(t^n, y - v\Delta t/2, v) - f(t^{n+1/2}, y, v)] dv \right| dy = \int \left| \int A(y, v) dv \right| dy
\end{aligned} \tag{7.128}$$

where $A(y, v) := f(t^n, y - v\Delta t/2, v) - f(t^{n+1/2}, y, v)$, the inequality coming from $\|K\|_{L^\infty([0,1])} \leq 1$. Denoting respectively $t_s := t^n + \Delta t/2 - s$ and $y_s(v) := y - vs$ for concise notations, we then observe that

$$\begin{aligned}
A(y, v) &= \int_0^{\Delta t/2} \frac{d}{ds} f(t_s, y_s(v), v) ds \\
&= \int_0^{\Delta t/2} -(\partial_t f + v\partial_x f)(t_s, y_s(v), v) ds \\
&= \int_0^{\Delta t/2} B(s, y, v) ds,
\end{aligned}$$

with $B(s, y, v) := -E(t_s, y_s(v))\partial_v f(t_s, y_s(v), v)$, this last equality coming from the Vlasov equation. Now, instead of writing a direct majoration that would give $|\mathcal{E}_3| \leq C(T)\Delta t$ (which is not enough), we integrate by parts

$$\begin{aligned}
\int s\partial_x E(t_s, y_s(v))f(t_s, y_s(v), v) dv &= - \int \frac{d}{dv} [\partial_x E(t_s, y_s(v))] f(t_s, y_s(v), v) dv \\
&= \int E(t_s, y_s(v)) \frac{d}{dv} [f(t_s, y_s(v), v)] dv \\
&= \int E(t_s, y_s(v)) \cdot (-s\partial_x f + \partial_v f)(t_s, y_s(v), v) dv,
\end{aligned}$$

which yields

$$\begin{aligned}
\int B(s, y, v) dv &= -s \int [\partial_x E(t_s, y_s(v))f(t_s, y_s(v), v) \\
&\quad + E(t_s, y_s(v))\partial_x f(t_s, y_s(v), v)] dv.
\end{aligned}$$

From lemma 2.3, it is then seen that

$$\begin{aligned}
\left| \int A(y, v) dv \right| &= \left| \int \int_0^{\Delta t/2} B(s, y, v) ds dv \right| \leq \Delta t \sup_{|s| \leq \Delta t} \left| \int B(s, y, v) dv \right| \\
&\leq \Delta t^2 \int_{-Q(T)}^{Q(T)} C(T) dv \leq C(T)\Delta t^2,
\end{aligned}$$

which together with (7.128) yields $|\mathcal{E}_3| \leq C(T)\Delta t^2$. For the fourth term, we finally have

$$\begin{aligned}\mathcal{E}_4 &= V(t^{n+1}) - V(t^{n+1/2}) + V(t^{n+1/2}) - V(t^n) - \Delta t E_X(t^{n+1/2}) \\ &= \int_0^{\Delta t/2} [E_X(t^{n+1} - t) + E_X(t^n + t)] dt - \Delta t E_X(t^{n+1/2}) \\ &= \int_0^{\Delta t/2} [E_X(t^{n+1} - t) - E_X(t^{n+1/2}) + E_X(t^n + t) - E_X(t^{n+1/2})] dt \\ &= \int_0^{\Delta t/2} \int_t^{\Delta t/2} [\dot{E}_X(t^{n+1} - s) - \dot{E}_X(t^n + s)] ds dt,\end{aligned}$$

which yields

$$|\mathcal{E}_4| \leq \Delta t^3 \|\ddot{E}_X\|_{L^\infty([0, T])} \leq C(T)\Delta t^3$$

according to (7.127), and the proof is complete. \square

7.2 Proof of lemma 4.10

Recalling that the construction of $\mathbb{T}(M, \mathcal{F})$ makes use of the backward level ℓ^* defined in (3.33), it is readily seen that any cell α in the intermediate (non graded) mesh $\tilde{\mathbb{T}}(M, \mathcal{F})$ satisfies

$$\ell^*(M, \mathcal{F}, \alpha) \leq \ell(\alpha). \quad (7.129)$$

This in fact also holds for the cells of $\mathbb{T}(M, \mathcal{F})$. For proving this, let α be a cell of $\mathbb{T}(M, \mathcal{F}) \setminus \tilde{\mathbb{T}}(M, \mathcal{F})$, and denote by $\tilde{\alpha}$ its unique ancestor that belongs to $\tilde{\mathbb{T}}(M, \mathcal{F})$. Writing

$$\begin{aligned}(x^*, v^*) &:= \mathcal{F}^{-1}(c_\alpha) = (x_\alpha, v_\alpha - G(x_\alpha)) \\ (\tilde{x}^*, \tilde{v}^*) &:= \mathcal{F}^{-1}(c_{\tilde{\alpha}}) = (x_{\tilde{\alpha}}, v_{\tilde{\alpha}} - G(x_{\tilde{\alpha}})),\end{aligned} \quad (7.130)$$

we must show that any $\eta \in M$ containing (x^*, v^*) satisfies

$$\ell(\eta) \leq \ell(\alpha), \quad (7.131)$$

while it is readily seen from (7.129) applied to $\tilde{\alpha}$ that any $\tilde{\eta} \in M$ containing $(\tilde{x}^*, \tilde{v}^*)$ satisfies

$$\ell(\tilde{\eta}) \leq \ell(\tilde{\alpha}). \quad (7.132)$$

According to (7.130), we first have

$$x^* = x_\alpha \in \alpha_x \subset \tilde{\alpha}_x \subset \tilde{\eta}_x, \quad (7.133)$$

where we have used (7.132) for the last inclusion. Observing that

$$\max(|x_{\tilde{\alpha}} - x_\alpha|, |v_{\tilde{\alpha}} - v_\alpha|) \leq (2^{-\ell(\tilde{\alpha})} - 2^{-\ell(\alpha)})/2,$$

we compute

$$\begin{aligned}|\tilde{v}^* - v^*| &\leq |v_{\tilde{\alpha}} - v_\alpha| + |G(x_{\tilde{\alpha}}) - G(x_\alpha)| \\ &\leq |v_{\tilde{\alpha}} - v_\alpha| + |x_{\tilde{\alpha}} - x_\alpha|/2 \\ &\leq (2^{-\ell(\tilde{\alpha})} - 2^{-\ell(\alpha)}) \cdot 3/4 \\ &< 2^{-\ell(\tilde{\alpha})} (1 - 2^{-(\ell(\alpha) - \ell(\tilde{\alpha}))}) \\ &< 2^{-\ell(\tilde{\eta})} (1 - 2^{-(\ell(\alpha) - \ell(\tilde{\alpha}))}),\end{aligned} \quad (7.134)$$

where the second inequality comes from (4.83) and the last one comes from (7.132). In some sense, the relations (7.133) and (7.134) express that η is ‘not too far’ from $\tilde{\eta}$. And we can observe that the level of η is maximal when the gradation of M is saturated around $\tilde{\eta}$: more precisely, because (7.134) reads

$$2^{\ell(\tilde{\eta})}|\tilde{v}^* - v^*| < \frac{1}{2} + \frac{1}{4} + \cdots + \frac{1}{2^{\ell(\alpha) - \ell(\tilde{\alpha})}},$$

we can check on figure 9 that we have $\ell(\eta) \leq \ell(\tilde{\eta}) + \ell(\alpha) - \ell(\tilde{\alpha})$. Together with (7.132), this finally yields (7.131).

Now let (x, v) be such that $\mathcal{F}(x, v) \in \alpha$. The game now consists of showing that (x, v) is ‘not too far’ from the cell η defined above. Clearly, we have

$$x \in \alpha_x \quad \text{and} \quad |v + G(x) - v_\alpha| \leq 2^{-\ell(\alpha)}/2, \quad (7.135)$$

and it follows from the previous discussion that $\alpha_x \subset \eta_x$, so that

$$x \in \eta_x. \quad (7.136)$$

Using again (4.83), we then compute

$$\begin{aligned} |v - v^*| &= |v - v_\alpha + G(x_\alpha)| \\ &\leq |v + G(x) - v_\alpha| + |G(x_\alpha) - G(x)| \\ &\leq (2^{-\ell(\alpha)} + |x_\alpha - x|)/2 \\ &\leq 2^{-\ell(\alpha)} \cdot 3/4 \\ &\leq 2^{-\ell(\eta)} \cdot 3/4, \end{aligned} \quad (7.137)$$

where the last inequality again comes from (7.131). Since any cell $\beta \in B(M, \mathcal{F}, \alpha)$ contains (x, v) , we can verify that $\#(B(M, \mathcal{F}, \alpha))$ is maximal when the gradation of the mesh is saturated around η , which is again the configuration represented on figure 9 (with $\tilde{\eta}$, \tilde{x}^* and \tilde{v}^* now replaced by η , x^* and v^*). Combining this observation with (7.136) and (7.137), we find that any such β must be drawn in solid lines on this figure, which makes (4.84) obvious (a closer, yet tedious look shows that the optimal constant is 7). We also clearly have $\ell(\beta) \leq \ell(\eta) + 2$, and property (4.85) follows then from (7.131). \square

7.3 Proof of lemma 4.12

In order to prove lemma 4.12, we let, for a given cell $\beta \in M$,

$$\tilde{F}(M, \mathcal{F}, \beta) = \{ \alpha \in \tilde{\mathbb{T}}(M, \mathcal{F}), \mathcal{F}^{-1}(c_\alpha) \in \beta \}$$

be the cells of the intermediate (non graded) mesh $\tilde{\mathbb{T}}(M, \mathcal{F})$ whose center is backward advected into β . According to the construction of $\tilde{\mathbb{T}}(M, \mathcal{F})$, it is readily seen that

$$\ell(\beta) \leq \ell(\alpha), \quad \text{for any } \beta \in M, \quad \alpha \in \tilde{F}(M, \mathcal{F}, \beta). \quad (7.138)$$

The following lemma states an inverse inequality, which allows to bound the cardinality of the sets $\tilde{F}(M, \mathcal{F}, \beta)$.

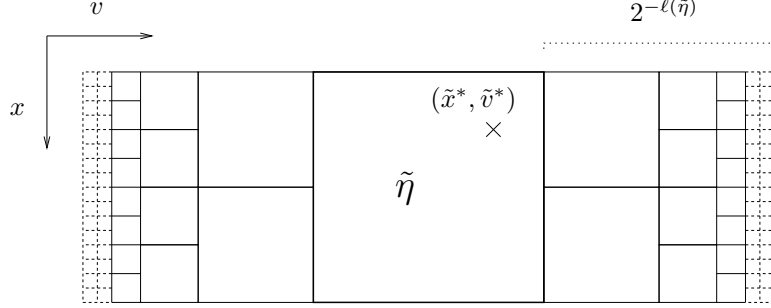


Figure 9: maximal change of resolution in a graded mesh.

Lemma 7.1. *Provided the advection field satisfies (4.83), we have*

$$\ell(\alpha) \leq \ell(\beta) + 1, \quad \text{for any } \beta \in M, \quad \alpha \in \tilde{F}(M, \mathcal{F}, \beta) \quad (7.139)$$

and there is a constant C such that

$$\sup_{\beta \in M} \#(\tilde{F}(M, \mathcal{F}, \beta)) \leq C \quad (7.140)$$

for any graded mesh M .

Proof. Given the generic form (4.74) of \mathcal{F} , $\mathcal{F}^{-1}(c_\alpha) \in \beta$ reads

$$x_\alpha \in \beta_x \quad (7.141)$$

$$v_\alpha - G(x_\alpha) \in \beta_v \quad (7.142)$$

and from (7.138), we see that (7.141) implies $\alpha_x \subset \beta_x$. Now according to the construction of the mesh $\mathbb{T}(M, \mathcal{F})$, we observe that the parent cell $\tilde{\alpha}$ of α is such that some $\tilde{\beta} \in M$ satisfies

$$\mathcal{F}^{-1}(c_{\tilde{\alpha}}) \in \tilde{\beta} \quad (7.143)$$

and $\ell(\tilde{\beta}) \geq \ell(\tilde{\alpha}) + 1 = \ell(\alpha)$, hence

$$\ell(\tilde{\beta}) \geq \ell(\beta). \quad (7.144)$$

Considering the dyadic structure of the cells, either α and β have same level and (7.139) is true, or $\ell(\alpha) \geq \ell(\beta) + 1$ and then the inclusion $\alpha_x \subset \beta_x$ leads to $\tilde{\alpha}_x \subset \beta_x$. Now from (7.143) we have $x_{\tilde{\alpha}} \in \tilde{\beta}_x$, and therefore

$$\tilde{\beta}_x \subset \beta_x. \quad (7.145)$$

This inclusion permits reasoning in the v direction only: we indeed observe that the graded structure of M prevents v_β and $v_{\tilde{\beta}}$ to be arbitrarily close. More precisely, we can verify that

$$|v_\beta - v_{\tilde{\beta}}| \geq \sum_{\ell=\ell(\beta)}^{\ell(\tilde{\beta})} 2^{-\ell} - 1/2 \cdot (2^{-\ell(\beta)} + 2^{-\ell(\tilde{\beta})}) = 3/2 \cdot 2^{-\ell(\beta)} (1 - 2^{-k})$$

where $k := \ell(\tilde{\beta}) - \ell(\beta)$. On the other hand, $\tilde{\alpha}$ being the parent cell of α , we observe that the stability condition (4.83) yields

$$|v_\alpha - v_{\tilde{\alpha}}| + |G(x_{\tilde{\alpha}}) - G(x_\alpha)| \leq 1/2 \cdot 2^{-\ell(\alpha)}(1 + \|G'\|_{L^\infty}) \leq 3/4 \cdot 2^{-\ell(\alpha)},$$

so that we have

$$\begin{aligned} |v_\beta - v_{\tilde{\beta}}| &\leq |v_\beta - v_\alpha + G(x_\alpha)| + |v_\alpha - v_{\tilde{\alpha}}| + |G(x_{\tilde{\alpha}}) - G(x_\alpha)| + |v_{\tilde{\beta}} - v_{\tilde{\alpha}} + G(x_{\tilde{\alpha}})| \\ &\leq 1/2 \cdot 2^{-\ell(\beta)} + 3/4 \cdot 2^{-\ell(\alpha)} + 1/2 \cdot 2^{-\ell(\tilde{\beta})} \leq 1/2 \cdot 2^{-\ell(\beta)}(1 + 3/4 + 2^{-k}), \end{aligned}$$

where the second inequality comes from the above observation combined with (7.142) and (7.143), and the third one from (7.138). It follows that $3(1 - 2^{-k})$ is not larger than $7/4 + 2^{-k}$, which leads to $k < 2$, hence (7.139) is proved. From (7.141)-(7.142), using again condition (4.83), we also have

$$\begin{aligned} |x_\alpha - x_\beta| &\leq 1/2 \cdot 2^{-\ell(\beta)} \\ |v_\alpha - v_\beta - G(x_\beta)| &\leq |v_\alpha - G(x_\alpha) - v_\beta| + 1/2|x_\alpha - x_\beta| \leq 3/4 \cdot 2^{-\ell(\beta)}, \end{aligned}$$

and this together with (7.139) clearly implies (7.140) (with $C = 6$). \square

We shall now prove lemma 4.12. Since every cell α in $\tilde{\mathbb{T}}(M, \mathcal{F})$ obviously belongs to at least one set $\tilde{F}(M, \mathcal{F}, \beta)$, above lemma 7.1 gives

$$\#\tilde{\mathbb{T}}(M, \mathcal{F}) \leq \bigcup_{\beta \in M} \#\tilde{F}(M, \mathcal{F}, \beta) \leq C\#(M),$$

and (4.86) follows from remark 3.1.

Acknowledgments

The authors would like to thank their respective PhD advisors Albert Cohen and Eric Sonnendrücker for their continued support and the many helpful suggestions that made this article possible.

References

- [1] A. Arsen'ev. Global existence of a weak solution of Vlasov's system of equations. *U.S.S.R. Comp. Math. Math. Phys.*, 15(1):131–143, 1975.
- [2] C. Bardos and P. Degond. Global existence for the Vlasov-Poisson equation in 3 space variables with small initial data. *Ann. Inst. H. Poincaré Anal. Non Linéaire*, 2(2):101–118, 1985.
- [3] J. Batt. Global symmetric solutions of the initial value problem of stellar dynamics. *J. Differential Equations*, 25(3):342–364, 1977.
- [4] M. Berger and J. Olinger. Adaptive mesh refinement for hyperbolic partial differential equations. *J. Comput. Phys.*, 53(3):484–512, 1984.
- [5] M.J. Berger and P. Colella. Local adaptive mesh refinement for shock hydrodynamics. *J. Comput. Phys.*, 82(1):64–84, 1989.

- [6] N. Besse. Convergence of a semi-Lagrangian scheme for the one-dimensional Vlasov-Poisson system. *SIAM J. Numer. Anal.*, 42(1):350–382 (electronic), 2004.
- [7] N. Besse, F. Filbet, M. Gutnic, I. Paun, and E. Sonnendrücker. An adaptive numerical method for the Vlasov equation based on a multiresolution analysis. In F. Brezzi, A. Buffa, S. Escorsaro, and A. Murli, editors, *Numerical Mathematics and Advanced Applications ENUMATH 2001*, pages 437–446. Springer, 2001.
- [8] P. Binev, W. Dahmen, and R. DeVore. Adaptive finite element methods with convergence rates. *Numer. Math.*, 97(2):219–268, 2004.
- [9] C.K. Birdsall and A.B. Langdon. *Plasma Physics via Computer Simulation*. McGraw-Hill, New York, 1985.
- [10] M. Campos Pinto. A total curvature diminishing property for P_1 finite element interpolation. To appear in *Mathematisches Forschungsinstitut Oberwolfach Report*, 34/2004.
- [11] M. Campos Pinto and M. Mehrenberger. Adaptive numerical resolution of the Vlasov equation. To appear in *Numerical methods for hyperbolic and kinetic problems, CEMRACS 2003/IRMA Lectures in Mathematics and Theoretical Physics*.
- [12] C.Z. Cheng and G. Knorr. The integration of the Vlasov equation in configuration space. *J. Comput. Phys.*, 22:330–351, 1976.
- [13] G. Chiavassa and R. Donat. Point value multiscale algorithms for 2D compressible flows. *SIAM J. Sci. Comput.*, 23(3):805–823 (electronic), 2001.
- [14] P.G. Ciarlet. Basic error estimates for elliptic problems. In *Handbook of numerical analysis, Vol. II*, Handb. Numer. Anal., II, pages 17–351. North-Holland, Amsterdam, 1991.
- [15] A. Cohen. *Numerical analysis of wavelet methods*, volume 32 of *Studies in Mathematics and its Applications*. North-Holland Publishing Co., Amsterdam, 2003.
- [16] A. Cohen, S.M. Kaber, S. Müller, and M. Postel. Fully adaptive multiresolution finite volume schemes for conservation laws. *Math. Comp.*, 72(241):183–225 (electronic), 2003.
- [17] J. Cooper and A. Klimas. Boundary value problems for the Vlasov-Maxwell equation in one dimension. *J. Math. Anal. Appl.*, 75(2):306–329, 1980.
- [18] W. Dahmen. Adaptive approximation by multivariate smooth splines. *J. Approx. Theory*, 36(2):119–140, 1982.
- [19] W. Dahmen. Wavelet and multiscale methods for operator equations. *Acta Numerica*, 6:55–228, 1997.
- [20] W. Dahmen, B. Gottschlich-Müller, and S. Müller. Multiresolution schemes for conservation laws. *Numer. Math.*, 88(3):399–443, 2001.

- [21] W. Dahmen, S. Müller, and T. Schlinkmann. On an adaptive multi-grid solver for convection-dominated problems. *SIAM J. Sci. Comput.*, 23(3):781–804 (electronic), 2001.
- [22] R. DeVore. Nonlinear approximation. *Acta Numerica*, 7:51–150, 1998.
- [23] F. Filbet and E. Sonnendrücker. Numerical methods for the Vlasov equation. In F. Brezzi, A. Buffa, S. Escorsaro, and A. Murli, editors, *Numerical Mathematics and Advanced Applications ENUMATH 2001*. Springer, 2001.
- [24] R.T. Glassey. *The Cauchy problem in kinetic theory*. Society for Industrial and Applied Mathematics (SIAM), Philadelphia, PA, 1996.
- [25] M. Gutnic, M. Haefele, I. Paun, and E. Sonnendrücker. Vlasov simulations on an adaptive phase-space grid. *Comput. Phys. Comm*, 164:214–219, 2004.
- [26] A. Harten. Adaptive multiresolution schemes for shock computations. *J. Comput. Phys.*, 115(2):319–338, 1994.
- [27] A. Harten. Multiresolution algorithms for the numerical solution of hyperbolic conservation laws. *Comm. Pure Appl. Math.*, 48(12):1305–1342, 1995.
- [28] E. Horst. On the classical solutions of the initial value problem for the unmodified nonlinear Vlasov equation. I. General theory. *Math. Methods Appl. Sci.*, 3(2):229–248, 1981.
- [29] E. Horst. On the classical solutions of the initial value problem for the unmodified nonlinear Vlasov equation. II. Special cases. *Math. Methods Appl. Sci.*, 4(1):19–32, 1982.
- [30] S. V. Iordanski. The Cauchy problem for the kinetic equation of plasma. *Amer. Math. Soc. Transl. Ser. 2*, 35:351–363, 1964.
- [31] P.-L. Lions and B. Perthame. Propagation of moments and regularity for the 3-dimensional Vlasov-Poisson system. *Invent. Math.*, 105(2):415–430, 1991.
- [32] J. Nečas. *Les méthodes directes en théorie des équations elliptiques*. Masson et Cie, Éditeurs, Paris, 1967.
- [33] A. Rault, G. Chiavassa, and R. Donat. Shock-vortex interactions at high Mach numbers. *J. Sci. Comput.*, 19(1-3):347–371, 2003. Special issue in honor of the sixtieth birthday of Stanley Osher.
- [34] P.-A. Raviart. An analysis of particle methods. In *Numerical methods in fluid dynamics (Como, 1983)*, volume 1127 of *Lecture Notes in Math.*, pages 243–324. Springer, Berlin, 1985.
- [35] O. Roussel, K. Schneider, A. Tsigulin, and H. Bockhorn. A conservative fully adaptive multiresolution algorithm for parabolic PDEs. *J. Comput. Phys.*, 188(2):493–523, 2003.
- [36] J. Schaeffer. Global existence of smooth solutions to the Vlasov-Poisson system in three dimensions. *Comm. Partial Differential Equations*, 16(8-9):1313–1335, 1991.

- [37] E. Sonnendrücker, F. Filbet, A. Friedman, E. Oudet, and J.L. Vay. Vlasov simulation of beams with a moving grid. *Comput. Phys. Comm.*, 164:390–395, 2004.
- [38] E. Sonnendrücker, J. Roche, P. Bertrand, and A. Ghizzo. The semi-Lagrangian method for the numerical resolution of the Vlasov equation. *J. Comput. Phys.*, 149(2):201–220, 1999.
- [39] H. Yserentant. Hierarchical bases. In *ICIAM 91 (Washington, DC, 1991)*, pages 256–276. SIAM, Philadelphia, PA, 1992.